NOTE TO USERS

Design of A Real-Time Process Control System

Shuo Liu

Electrical and Computer Engineering Department

McGill University, Montreal

2003.10

A thesis submitted to McGill University
in partial fulfillment of the requirements
of the degree of M.Eng.

Your file Votre référence
ISBN: 0-612-98550-4
Our file Notre référence
ISBN: 0-612-98550-4

Index

Abstract

This thesis presents the whole real-time decoupling control system design procedures for the water level and temperature control of the Feedback experimental process testbed Procon 38-003 using RT-Lab computer control system. First, the thesis describes the configuration of the system under study. Two approaches of modeling a shell-tube heat exchanger and a method to analyze a water tank system are presented with the linearization method applied on the derived MIMO process model. The control methods attempted on the plant are decoupling control scheme using *Decoupling Network* and *Relative Gain Array* pairing method. Applications and feasibility of the attempted control schemes are discussed. Then, description of the utilized hardware and software in the control system is presented. The emphasis is on the RT-Lab system, which acts as the core component in the whole system, and the signal converters, which are designed and implemented. Development and setup of the RT-Lab model is depicted in the sixth chapter. Merits and limitations of the designed control system are presented in the conclusion of this thesis through experimental records and written work.

I would like to express my sincere appreciation to Professor Benoit Boulet's valuable instructions and precious support on my graduate studies, especially during my research period on this thesis. Also, I want to acknowledge Professor Boulet for his thorough accuracy review of this thesis. In addition, I would like to express my gratitude to my co-supervisor Hannah Michalska.

Chapter 1 Introduction

"God must have been a control engineer, for the human body is replete with clever regulation and servo systems."

This sentence is quoted from Professor Pierre R. Bélanger's book *Control Engineering: A Modern Approach.* In our lives, automatic control plays such a vital role that no one can do without it. It is this idea that motivated me to choose System Control as my field of study. The importance of automatic control is reflected in the modern advances of engineering and science since the theory and practice of automatic control provide the means for attaining optimal performance of dynamic systems, and improving the productivity of industrial processes.

In many industrial operations, the control of water temperature and level is essential. This thesis demonstrates one approach of controlling these variables in a real-time manner. The plant under study is the process control training system *Procon 38-003* made by Feedback, which is shown in the following figure 1.1.

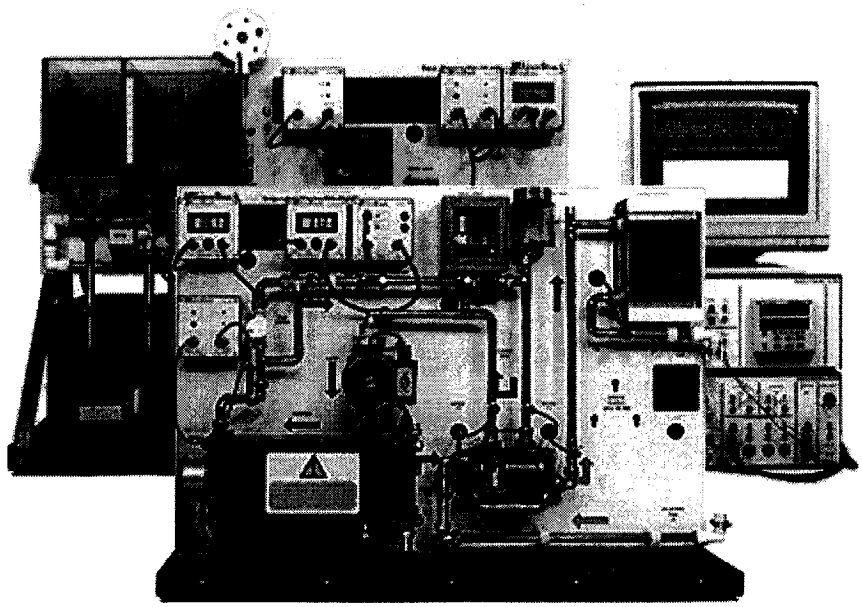

Figure 1.1 Procon 38-003

The goal of this thesis project is to control the tank's water temperature using a heat exchanger and its water level with Opal-RT's real-time control system *RT-Lab*. An Allen Bradley 1746 Open Controller and two signal converters, which were designed and implemented by the author, are also used and integrated into the overall control system.

Chapter 2 Literature Review

This chapter will present the theoretical background and a brief review of the reference material. The topics covered are Linear Dynamic Systems, Real-Time Control System, Multivariable Decoupling Control, Heat Transfer and Heat Exchanger.

2.1 Linear Dynamical Systems

In this section, we review some notions and results on linear system from the lecture notes of the course Linear System taught by Professor Benoit Boulet at McGill University [2]

Let a finite dimensional linear time-invariant dynamical system be described by the following linear constant coefficient equations:

$$\dot{x}(t) = Ax(t) + Bu(t) \qquad x(t_0) = x_0 \tag{2.1}$$

$$y(t) = Cx(t) + Du(t) \tag{2.2}$$

where $x(t) \in \mathbb{R}^n$ is called the system state, $x(t_0)$ is the initial condition of the system and $u(t) \in \mathbb{R}^m$ is the system input, and $y(t) \in \mathbb{R}^p$ is the system output. A, B, C and D are real constant matrices with appropriate dimensions. A dynamical system with m = 1 and p = 1 is know as a single-input, single-output (SISO) system; otherwise, it is called a multiple-input and multiple-output (MIMO) system. In this thesis, we shall be concerned mainly with MIMO systems.

For the given initial condition $x(t_0)$ and the input $u(t)$, the dynamical system will have its solution, or response $x(t)$ and $y(t)$ for $t \geq t_0$, which can be obtained from the following formulas:

$$x(t) = e^{A(t-t_0)}x(t_0) + \int_{t_0}^{t} e^{A(t-\tau)}Bu(\tau)d\tau \tag{2.3}$$

$$y(t) = Cx(t) + Du(t) \tag{2.4}$$

The matrix exponential e^{At} in (2.3) is defined by

$$e^{At} = I + At + \frac{1}{2!}A^2t^2 + \frac{1}{3!}A^3t^3 + \cdots \tag{2.4}$$

and it can also be calculated by

$$e^{At} = L^{-1}\{(sI - A)^{-1}\} \tag{2.5}$$

where L^{-1} stands for the inverse Laplace transform.

In the case of $u(t) = 0, \forall t \geq t_0$, it is easy to see from the solution (2.3) that for any $t_1 \geq t$ and $t \geq t_0$, we have

$$x(t) = e^{A(t-t_1)}x(t_1) \tag{2.6}$$

Therefore, the matrix function $\Phi(t,t_1) = e^{A(t-t_1)}$ acts as a transformation from one state to another, and thus $\Phi(t,t_1)$ is usually called the state transition matrix. The state of a linear system at one time can be obtained from the state at another time through the transition matrix.

The second property of linear dynamical system to be reviewed here is Controllability. For a Linear dynamical system, state x_0 is said to be controllable at time t_0 if for some finite time $t_1 \geq t_0$, there exists an input u that transfers the state $x(t)$ from x_0 at t_0 to the origin at t_1. ([2] Benoit Boulet), i.e., the dynamical system is said to be controllable if there exists an input u, which transfers the initial state x_0 to any desired state x_1. The controllability of a linear time-invariant dynamical system can be revealed by its controllability matrix, which is defined as:

$$Q_c := [\, B \; AB \; A^2B \; \cdots \; A^{n-1}B \,]$$

When Q_c has full row rank, the system is controllable.

2.2 Real-Time Control System

In our daily lives, real-time control systems can be found almost everywhere. Examples of real-time systems can be found in anti-lock braking controller in automobiles, automatic pilots in airplanes, network and telephone switching systems, robotic controllers and many industrial applications. Figure 2.1 shows a model of a real-time system.

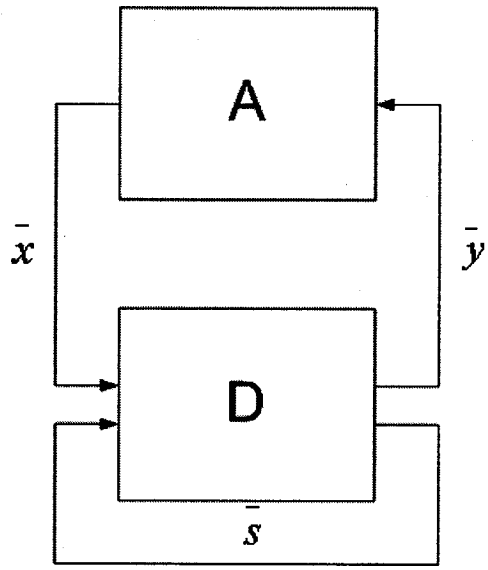

Figure 2.1 Real-Time system Model

A real-time system has a decision component that interacts with the external environment by taking sensor readings and computing control decisions. The model can be characterized by the following components.

Sensor Vector	$\bar{x} \in X$
Decision Vector	$\bar{y} \in Y$
System State Vector	$\bar{s} \in S$
Environmental Constraints	A
Decision Map	$D, D : S \times X \rightarrow S \times Y$
Timing Constraints	T

In these components, X is the space of sensor reading values, Y is the space of decision values, and S is the space of system state values. In addition, the environmental constraints A are relationships over X, Y, S.

The decision map D determines the next decisions and system state values with the current system state and sensor inputs. Decision maps can be implemented by computer system, which consists of a network of distributed monitoring and decision-making subsystems. The implementation of the decision map D is subject to a set of timing constraints T, which are about how fast the map D should be performed.

A typical computer-controlled real-time system can be schematically described in Figure 2.2.

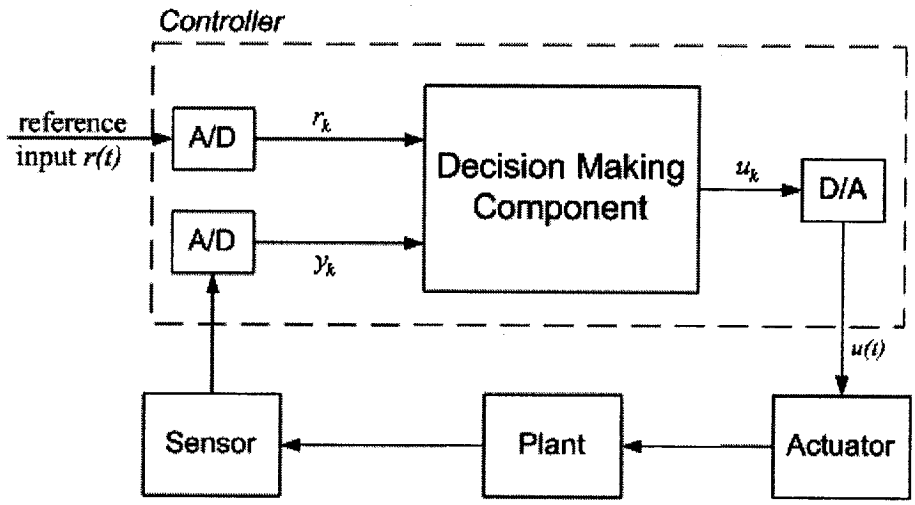

Figure 2.2 Computer Controlled Real-Time System

In the above block diagram ([5] Jane W.S. Liu), the state of the plant is monitored by sensors and can be changed by actuators. The real-time (computing) system estimates from the sensor readings and computes a control output based on the difference between the current state and the desired state (called *reference input* in the figure). The computing system is the decision-making component in the whole

control system. Output from the decision-making component activates the actuators, which bring the plant closer to the desired state.

The design of a real-time system consists of several steps. The first step is to construct a model of the system to be studied. This model should carry out simulated executions of the simulated system and display the outcomes of these executions. In another words, we can predict the performance of the real system with the built model. For instance, a computer model can be designed to simulate the behavior of an automobile crashing into a concrete barrier, showing its effects on the occupants of this automobile.

The procedure of applying executions on the model is the second step of building a real-time control system: simulation. Simulation is an efficient and safe way to study the behavior of the system and to study different ways of implementing the actual system. If we detect behavior or events that are inconsistent with the real physical system, we can revise the model. In the case in which we consider several models as possible ways to implement the actual system, we can select the model that best satisfies the specification and safety assertions. Simulation advances the analysis and building of the system model.

After running the simulation in a software environment, we can apply the controller on the real physical system. In this step, extra caution should be taken since unexpected behavior may be caused by events and actions that were not modeled.

2.3 Multivariable Decoupling Control

The study of decoupling linear time-invariant multivariable systems has received considerable attentions in both control theory and industrial practice for several decades. Typically, a system will have several variables to be controlled in which case it is called a multivariable system. The most important feature of a multivariable system is the possible cross-couplings or interactions between its variables, i.e., one input variable may affect some or all of the output variables. This prevents the control engineer from designing each loop independently since the adjustment of controller parameters of one of the loops typically affects the performance of other loops.

Dating back at least to 1938, researchers and engineers have come up with lots of approaches to implement decoupling control on multivariable systems. The decoupling methods applied in this thesis are the Relative Gain Array (RGA) (Bristol, 1966) ([3] Graham C. Goodwin) and Decoupling Network Method ([4] K. Warwick). Detailed descriptions of these methods will be presented in the fifth chapter of the thesis.

2.4 Heat Transfer and Heat Exchanger System

Heat is defined as the form of energy that is transferred between two systems (or a system and its surroundings) by temperature difference. We know from experience that a cup of hot water left on a table eventually cools down to room temperature. This physical phenomena shows that when a body is left in a medium which is at a different temperature, energy transfer takes place between the body and the surrounding medium until thermal equilibrium is established, i.e., the body and the medium reach the same temperature. ([6] Cengel).

The physical principle for the heat contained in a mass M of water is:

$$Q = MCT \tag{2.7}$$

where C in equation (2.7) denotes the Heat Capacity of water and T represents the temperature of water.

Heat can be transferred in three different ways: conduction, convection, and radiation. A detailed description of these heat transfer modes can be found in most textbooks on thermodynamics. The book that we mostly referred to is *Heat Transfer* ([7] J.P.Holman).

Convection is defined as the mode of energy transfer between a solid surface and the adjacent liquid or gas which is in motion. The rate of heat transfer by convection is determined from Newton's law of cooling, which is expressed as:

$$\dot{Q} = hA(T_s - T_f) \tag{2.8}$$

where h is the convection heat transfer coefficient, A is the surface area through which heat transfer takes place, T_s is the surface temperature and T_f is the fluid temperature.

Conduction is the transfer of energy from the more energetic particles of a substance to the adjacent less energetic ones as a result of interactions between the particles. Conduction can take place in solids, liquids, or gases. The rate of heat transfer by conduction is expressed as

$$\dot{Q} = k_t A \frac{dT}{dx} \tag{2.9}$$

which is known as Fourier's law.

With the knowledge of heat transfer, people have invented many devices. Heat exchanger is one of them. The heat exchanger is an apparatus that facilitates heat exchange among fluids with different temperatures, without direct contact between them. In a heat exchanger, two or more fluid streams are involved in the heat transfer process. Heat exchangers are used in several industrial applications, e.g.,

in the space shuttle, aircraft, automobile, electronic technology and chemical engineering.

According to the geometrical and operating characteristics, industrial heat exchangers can be classified into two groups ([8] Roetzel and Xuan): (1) recuperative heat exchangers; (2) regenerative heat exchangers. Recuperative heat exchangers refer to apparatus in which fluids are separated from each other by a solid wall and flow continuously. Heat is transferred from hot fluids to cold ones across the solid wall. If all operating conditions remain stable, a steady state can be reached in this type of heat exchangers. The heat exchanger being studied in this thesis is of this type. Regenerative heat exchangers have quite different structures and are composed of solid matrices. The heat exchange fluids flow over the same surface in a regenerator during separate time spans. While the hot fluid is flowing through the solid matrices (the hot period), the solid matrices absorb and store heat; during the cold fluid flow (the cold period) heat is transferred from the solid matrices to the cold fluid.

Recuperative heat exchangers exist in many different types. A common methodology is to classify recuperative exchangers into the tubular and plate types. To some extent, tubular exchangers imply shell-tube heat exchanger with a shell and tubes. This type of heat exchanger is applied in many industrial applications. There are two domains in a shell-tube heat exchanger: the "tubeside" domain commonly refers to the inside of the tubes while the "shellside" refers to the remaining space between the shell and tubes in the heat exchanger. Generally, two fluid streams flow through the shell-tube heat exchanger in an industrial operation. The shellside fluid flows through the space between the shell and tubes and the tubeside fluid flows inside the tubes. The tubeside stream may flow through all tubes in a parallel

connection and the total tubeside flow length equals the tube length. This flow arrangement is referred to as a single tubeside pass arrangement. The heat exchanger under study in this thesis is of this type. In the third chapter of this thesis, a more detailed description of shell-tube heat exchanger will be presented. The references of [8] and [9] were used to model and study the heat exchanger

Chapter 3 Process Control Training System *Procon 38-003*

For a better understanding of this thesis, it is necessary to describe the *Procon 38-003* process control training system. This chapter discusses the hardware configuration of the experimental setup. Some important devices mounted in it will be explained in details. The configuration of the *Procon 38-003* is shown in Figure 3.1 on the next page.

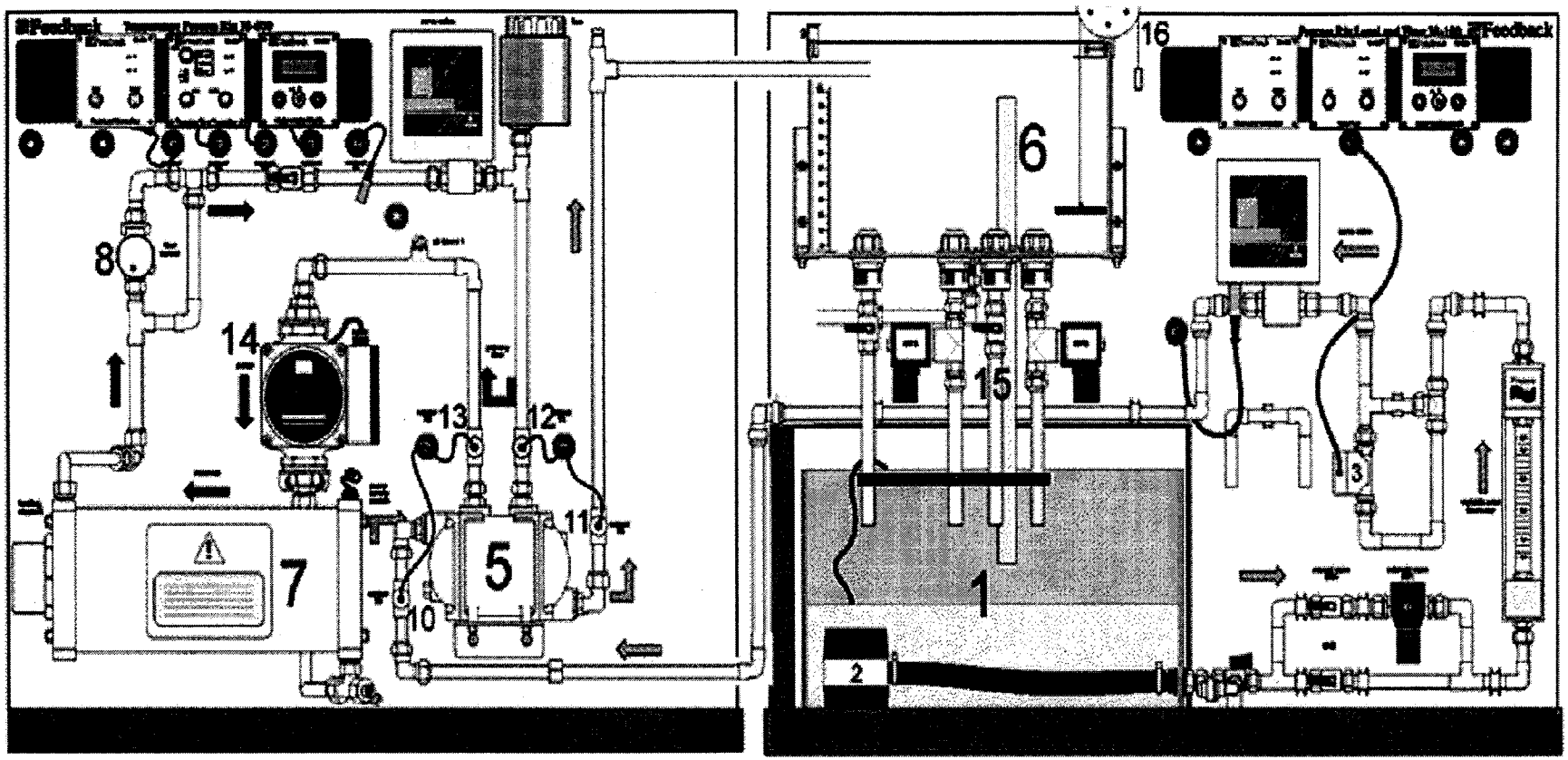

Figure 3.1 Procon 38-003 Proces Control Test Bed

In the *Procon 38-003*, there are two water circuits. Each of the circuits is marked out by either dark or grey arrows in Figure 3.1. The dark arrows refer to the primary flow while the gray arrows are for the secondary flow. Along the water flow circuits, there are numbered devices mounted in the Rig. Table 3.1 lists the names and functions of each of the devices.

Table 3.1

Part Number	Name	Function
1	Reservoir Tank	Reserves water for the use of the primary water flow
2	Primary Water Pump	Pumps the water in the primary circuit
3	Primary Flow Sensor	Measures primary water flow rate
4	Primary Servo	Controls primary water flow rate
5	Heat Exchanger	Exchanges heat between the primary and secondary water flows
6	Target Tank	Primary flow's final destination. The water level and temperature are the variables to be controlled.
7	Heater Tank	Heats the secondary water flow
8	Secondary Flow Sensor	Measures the water flow in the secondary water circuit
9	Secondary Servo	Controls secondary water flow rate
10-13	Temperature Sensor	Measures water temperature in the water pipes
14	Secondary Primary Water Pump	Pumps the secondary flow
15	Target Tank Orifice	Allows water to flow out of the Target Tank

For the primary flow, the water in the *Reservoir Tank* is pumped out by the *Primary Water Pump*. The flow rate of this water circuit is controlled by the *Primary Servo Valve*. Figure 3.2 shows the structure of this servo valve.

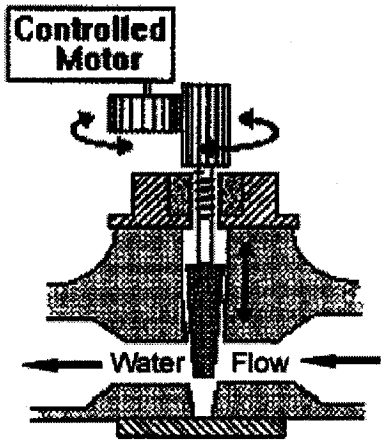

Figure 3.2 Servo Valve

Both the primary and secondary servo valves are of the same type. As illustrated in figure 3.2, there is a controlled motor regulating the opening of the valve and hence controlling the flow rate of the water passing through the valve. This valve is linearly controlled by a 4-20mA current signal.

After flowing through the servo valve, the water in the primary circulation makes its way into the heat exchanger.

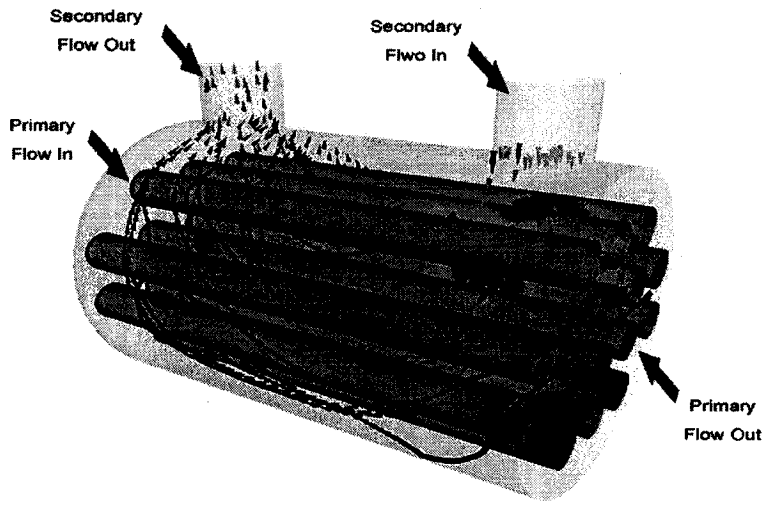

Figure 3.3 Counter Flow Shell-Tube Heat Exchanger

The heat exchanger is of Shell and Tube type. In the exchanger, hot water from the second circuit fills the shell and heats up the primary water flowing in the tubes. By adjusting the primary and secondary flow rates, we can achieve the objective of controlling the water temperature flowing out of the exchanger.

The Target Tank is the destination of the primary current. Water level and temperature in this tank are the variables to be controlled. Note that there are a number of pipes in the bottom of this tank. These allow the water to flow out of the tank. Each of the pipes has either a manual or a solenoid open-closed valve to control it.

Different from the primary water flow, the secondary flow is a closed circuit. Water in the *Heater Tank* is driven out of it by a pump and then flows into the heat exchanger. The flow rate of this circuit is controlled by the *Secondary Servo Valve*. In the heat exchanger, heat carried in the secondary flow is conducted to the primary flow through the tube metal. Cooled down by the heat transfer process, the secondary flow will go back to the *Heater Tank* and be warmed up again.

Chapter 4 Mathematical Modeling and Linearization of Dynamical Systems

The starting point for a control system design is to derive a mathematical model of the plant. A system may be represented in many different ways and, therefore may have many mathematical models. Depending on the particular system and the particular circumstances, one mathematical model may be better suited than other models. In our case, the heat exchanger is of dominant importance in the system model. Two modeling approaches for the heat exchanger will be illustrated in this chapter, although only one model is adopted for further control system design. The selection of the system model is based on the performance of each derived model and the control system requirement.

4.1 First Heat Exchanger Modeling Approach

Figure 4.1 shows the inner structure of the heat exchanger under study.

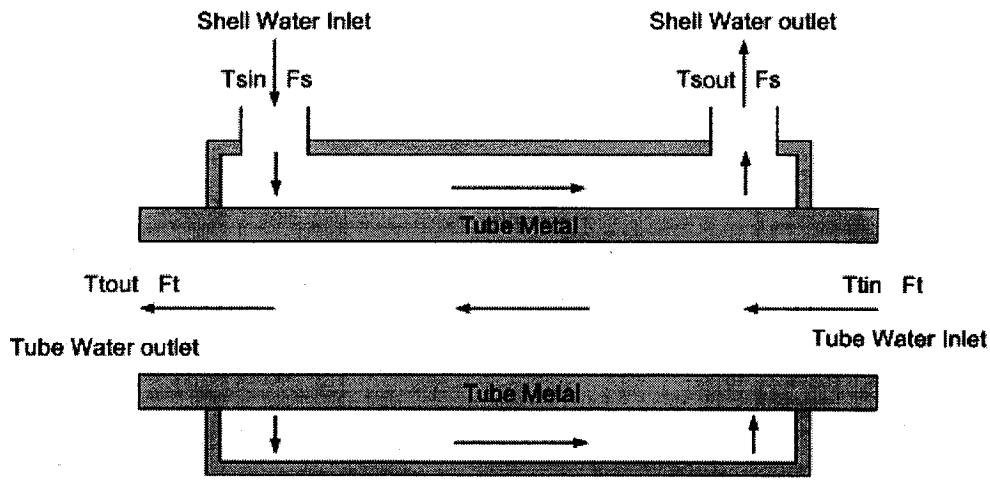

Figure 4.1 Inner Structure of the Heat Exchanger

There are two currents flowing through the heat exchanger. The primary circulation flows in the tubes and receives heat conducted from the secondary water circulation through the tube metal.

Table 4.1 describes the parameters used in figure 4.1.

Table 4.1

Parameter	Description
Tsin	Temperature of the water flowing into the shell of heat exchanger
Tsout	Temperature of the water flowing out of the shell of heat exchanger
Ttin	Temperature of the water flowing into the tube of heat exchanger
Ttout	Temperature of the water flowing out of the tube of heat exchanger
Fs	Flow rate of the water in the shell side of heat exchanger
Ft	Flow rate of the water in the tube side of heat exchanger

To facilitate the development of the heat exchanger's mathematical model, I have attempted to transform it into other physical systems, which are more straightforward to analyze. These transformations are based on keeping the physical properties of the initial system.

One representation of the heat exchanger system is by evenly dividing it into subsections and applying a series of water tanks to denote each subsection ([1] Pierre Bélanger]. The following figure shows one instance of such a representation. In this case, the exchanger has been divided into two subsections.

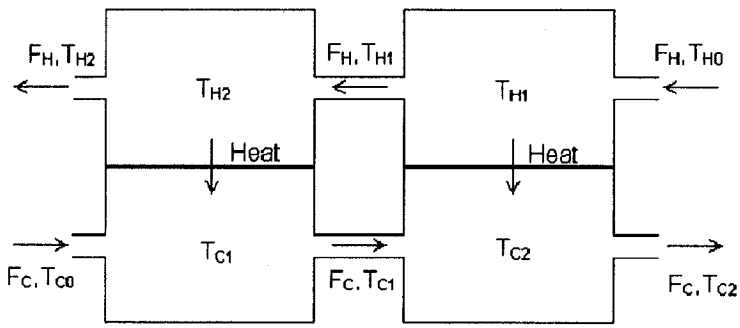

Figure 4.2 Equivalent Heat Exchanger System

Fc: Cold (primary) Water Flow Rate

Fh: Hot (secondary) Water Flow Rate

Tc1, Tc2: Cold (primary) Water Tank Temperature

Th1, Th2: Hot (secondary) Water Tank Temperature

Tc0, Th0: Initial Water Temperature

In the above water tank system, the secondary water circulation flows through the two upper tanks at a flow rate of Fh while the primary circulation water flows through the lower tanks at a flow rate of Fc. The heat transfers from the upper tanks into the lower tanks at the separating areas. Tc0 and Th0 represent the temperature of the water going into the tanks. These are constants when the heat exchanger is in use. Both of the flow rates can be adjusted by servo in *Procon 38-003*. The adjustment of these two flow rates varies the amount of heat being transferred. This results in a change in the exchanger outlet water temperature.

For the first water tank, the energy balance can be expressed by the following equation:

Energy Storage in Tank	**=**	***Energy Gained with Flow in and Flow out***	**+**	***Energy gained from conduction at the tank boundary area***

The physical principle for the heat contained in a mass M of water is:

$$Q = MCT \tag{4.1.1}$$

where C in equation (4.1.1) denotes the Heat Capacity (J/Kg* C°) of water and T represents the temperature (C°) of water. Therefore, the heat contained in the first cold water tank is:

$$Q_{C1} = \rho V_{C1} C T_{C1} \tag{4.1.2}$$

where:

ρ : Water Density (kg/m^3)

V_{C1} : Volume of the first Cold Water Tank (m^3)

T_{C1} : Average Water Temperature in First Cold Water Tank (C°)

During a time interval t to Δt, the mass of water flowing through the first cold water tank is:

$$M = \rho F_c \Delta t \tag{4.1.3}$$

where

F_c : Cold water flow rate (m^3/sec)
Δt : Time interval (sec)

Assume the water flowing into the tank is at temperature T_{C0} and the water flowing out of the tank is at temperature T_{C1}. The energy gained with the water flowing in and out of the tank can be expressed as:

$$\Delta Q_G = MCT = \rho F_C \Delta t C (T_{C0} - T_{C1}) \tag{4.1.4}$$

On the other hand, the heat conducted across the boundary between the last hot tank and the first cold tank is:

$$\Delta Q = k(T_{H2} - T_{C1})\Delta t \tag{4.1.5}$$

where

k Heat Conduction Coefficient (j/sec*C°)
Δt Time interval (sec)
T_{H2}, T_{C1} Average temperature of the second hot water tank and the first cold water tank (C°)

Since there is some heat loss during the heat transfer process, a coefficient α should be applied to Equation (4.1.5). This heat loss is from the radiation of the heat exchanger's outer shell. The α here is measured from experiments on the heat exchanger. This leads to the following result:

$$\Delta Q_C = \alpha k(T_{H2} - T_{C1})\Delta t \tag{4.1.6}$$

Applying (4.1.4) and (4.1.6) into the energy balance equation, the heat exchanging process can be expressed as the following:

$$Q_{C1} = \Delta Q_G + \Delta Q_C = \rho F_C \Delta t C(T_{C0} - T_{C1}) + \alpha k(T_{H2} - T_{C1})\Delta t \qquad (4.1.7)$$

Applying equation (4.1.2) into (4.1.7) and letting $\Delta t \to 0$, we can obtain the following differential equation:

$$\dot{T}_{C1} = \frac{1}{V_C} F_C T_{C0} - (\frac{F_C}{V_C} + \frac{\alpha k}{\rho V_C C}) T_{C1} + \frac{\alpha k}{\rho V_C C} T_{H2} \qquad (4.1.8)$$

At this point, the equation describing the energy transfer process in the first cold water tank is set up. In the same manner, equations for the other cold-water tank can be derived:

$$\dot{T}_{C2} = \frac{1}{V_C} F_C T_{C1} - (\frac{F_C}{V_C} + \frac{\alpha k}{\rho V_C C}) T_{C2} + \frac{\alpha k}{\rho V_C C} T_{H1} \qquad (4.1.9)$$

With equations (4.1.8) and (4.1.9), the mathematical modeling procedure for the primary water circuit is complete.

In contrast to the cold tanks, the hot water tanks have a different underlying heat exchange process. This results in a slightly different derivation of the differential equations for the hot water tanks.

The energy balance equation for the first hot water tank is:

Energy Storage in Tank	=	***Energy gain with Flow in and Flow out***	-	***Energy loss from conduction at the tank boundary area***

Similar to equation (4.1.2), the heat contained in the first hot water tank can be expressed as:

$$Q_{H1} = \rho V_{H1} C T_{H1} \qquad (4.1.10)$$

The energy gained with flow in and flow out of the first hot water tank is:

$$\Delta Q_G = \rho F_H \Delta t C(T_{H0} - T_{H1}) \qquad (4.1.11)$$

The energy loss from the conduction at the tank boundary area is:

$$\Delta Q_C = k(T_{H1} - T_{C2})\Delta t \tag{4.1.12}$$

Applying Equations (4.1.11) and (4.1.12) into the energy balance equation for the first hot water tank, we can derive the following result:

$$\Delta Q_{H1} = \Delta Q_G - \Delta Q_C = \rho F_H \Delta t C(T_{H0} - T_{H1}) - k(T_{H1} - T_{C2})\Delta t \tag{4.1.13}$$

Plugging (4.1.10) into (4.1.13) and letting $\Delta t \to 0$, we obtain the following equation:

$$\dot{T}_{H1} = \frac{1}{V_H} F_H T_{H0} - (\frac{F_H}{V_H} + \frac{k}{\rho V_H C}) T_{H1} + \frac{k}{\rho V_H C} T_{C2} \tag{4.1.14}$$

Similarly, the equation for the other hot water thank is derived as:

$$\dot{T}_{H2} = \frac{1}{V_H} F_H T_{H1} - (\frac{F_H}{V_H} + \frac{k}{\rho V_H C}) T_{H2} + \frac{k}{\rho V_H C} T_{C1} \tag{4.1.15}$$

To summarize, the mathematical model derived for the heat exchanger consists of the following four equations:

$$\dot{T}_{C1} = \frac{1}{V_C} F_C T_{C0} - (\frac{F_C}{V_C} + \frac{\alpha k}{\rho V_C C}) T_{C1} + \frac{\alpha k}{\rho V_C C} T_{H2} \tag{4.1.8}$$

$$\dot{T}_{C2} = \frac{1}{V_C} F_C T_{C1} - (\frac{F_C}{V_C} + \frac{\alpha k}{\rho V_C C}) T_{C2} + \frac{\alpha k}{\rho V_C C} T_{H1} \tag{4.1.9}$$

$$\dot{T}_{H1} = \frac{1}{V_H} F_H T_{H0} - (\frac{F_H}{V_H} + \frac{k}{\rho V_H C}) T_{H1} + \frac{k}{\rho V_H C} T_{C2} \tag{4.1.14}$$

$$\dot{T}_{H2} = \frac{1}{V_H} F_H T_{H1} - (\frac{F_H}{V_H} + \frac{k}{\rho V_H C}) T_{H2} + \frac{k}{\rho V_H C} T_{C1} \tag{4.1.15}$$

The state-space representation of this mathematical model can be derived using the relationships listed in table 4.2.

Table 4.2

Outputs	T_{C3}			
	y_1			
Inputs	F_C	F_H		
	u_1	u_2		
State Variable	T_{C1}	T_{C2}	T_{C3}	T_{H1}
	x_1	x_2	x_3	x_4

The state-space form of the mathematical model is:

$$\dot{x}_1 = u_1(A_3T_{C0} - A_3x_1) - (A_1x_1 - A_1x_4) \tag{4.1.16}$$

$$\dot{x}_2 = u_1(A_3x_1 - A_3x_2) - (A_1x_2 - A_1x_3) \tag{4.1.17}$$

$$\dot{x}_3 = u_2(A_4T_{H0} - A_4x_3) - (A_2x_3 - A_2x_2) \tag{4.1.18}$$

$$\dot{x}_4 = u_2(A_4x_3 - A_4x_4) - (A_2x_4 - A_2x_1) \tag{4.1.19}$$

where

$$A_1 = \frac{\alpha k}{\rho V_C C}, A_2 = \frac{k}{\rho V_C C}, A_3 = \frac{1}{V_C}, A_4 = \frac{1}{V_H}.$$

4.2 Second Heat Exchanger Modeling Approach

Recall the equivalent water tank system in the previous section. The following figure shows this system with two subsections.

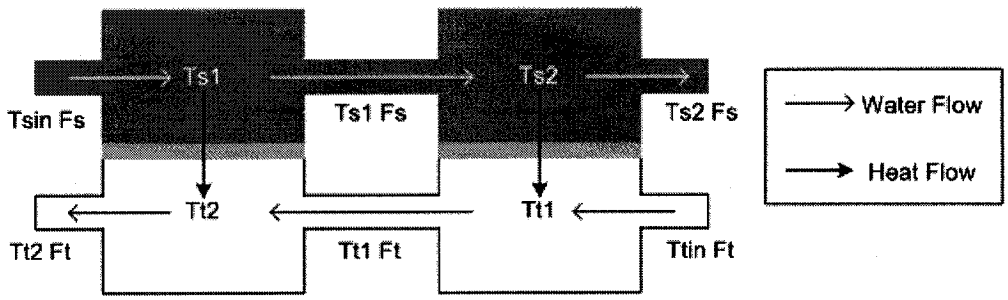

Figure 4.3 Equivalent Heat Exchanger System

Tsin	*Temperature of the water flowing into the exchanger's shell*
Ttin	*Temperature of the water flowing into the exchanger's tube*
Ts1, Ts2	*Temperature of the water in Shell subsection 1 and 2*
Tt1, Tt2	*Temperature of the water in Tube subsection 1 and 2*
Fs	*Flow rate of the water in exchanger's Shell*
Ft	*Flow rate of the water in exchanger's Tube*

In Figure 4.3, the dark gray shaded area represents the exchanger's shell subsections while the bottom white tanks represent the tube part. Different from Figure 4.2, the above diagram shows the tube metal part of the heat exchanger. This is represented by the light gray shaded areas in between the hot and cold water tanks in Figure 4.3.

The previous modeling approach only takes the shell side and tube side of the heat exchanger into consideration. The tube metal used to separate primary and secondary water flows is neglected. Since the Heat exchanger's tube metal is barely 1mm thick and its material is Cupro Nickel Alloy, which has very good thermal conductivity, the heat conduction process in tube metal can be ignored.

However, in most large-scale industrial shell-tube heat exchangers, the tube metal is too thick to be disregarded. This section will illustrate another modeling approach for the heat exchanger, which takes the tube metal into account.

To help develop the mathematical model for this system, we can transform the tank system into an equivalent electric circuit which is known as the thermo network. This is shown in Figure 4.4.

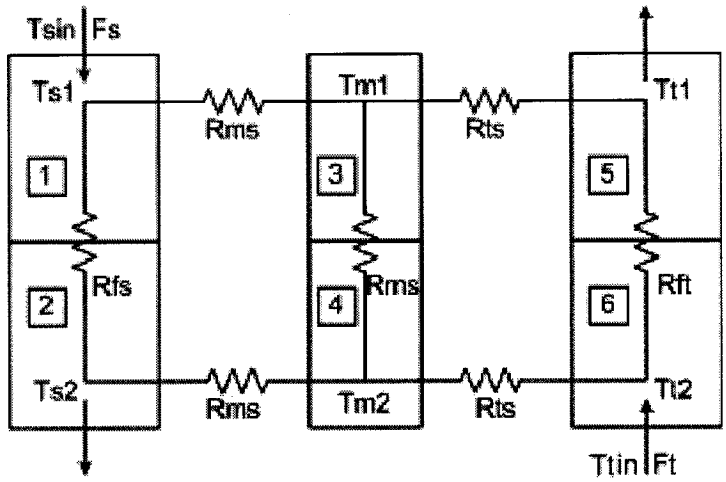

Figure 4.4 Electric Circuit Representation of the Heat Exchanger

The relationship between thermal and electric systems is summarized in Table 4.3

Table 4.3

Quantity	Electric System	Thermal System
Potential	Voltage (V)	Temperature difference (ΔT)
Flow	Current (I)	Heat Flux (Q)
Resistance	Resistance (R)	Potential/Flow ($\Delta T / Q$)
Capacitance	Capacitance ($C_E = \int I\, dt / V$ or $C_E(\frac{dV}{dt}) = I$)	Heat Capacitance ($C_T = \int Q\, dt / \Delta T$ or $C_T(\frac{dT}{dt}) = Q$)

Now the energy balance equation for a thermo system can be expressed as:

Rate of energy change in Thermo System	=	Net flow rate of energy into Thermo System	+	Internal energy generation rate in Thermo System

Therefore, for the i^{th} subsection of the heat exchanger, we have:

$$\rho CV_i \frac{dT_i}{dt} = \Sigma Q_{ij} + Q_i \tag{4.2.1}$$

where:

Q_{ij}: Net energy flow rate from Thermo System's j^{th} subsection to i^{th} subsection

V_i: Volume of the i^{th} subsection

T_i : Averager temperature of the Thermo system's i^{th} subsection

Q_i: Internal energy generation rate in Thermo System's i^{th} subsection

C Water heat capacity

ρ Water density

In (4.2.1),

$$Q_{ij} = \frac{(T_j - T_i)}{R_{ij}}$$

with

R_{ij} : Resistance between Thermo system's i^{th}subsection and j^{th} subsection

T_j : Temperature of the Thermo system's j^{th} subsection

T_i : Temperature of the Thermo system's i^{th} subsection

Thus, the Thermo Capacitance can be expressed as $C_{Ti} = \rho CV_i$. and equation (4.2.1) becomes:

$$C_{Ti} \frac{dT_i}{dt} = \Sigma \frac{T_j - T_i}{R_{ij}} + Q_i \tag{4.2.2}$$

4.2.1 Shell Side Energy Balance Relationship of the i^{th} Subsection

Let us assume the exchanger is divided into N subsections. Then, the energy balance for the i^{th} shell subsection can be expressed as the following:

Rate of energy storage in subsection	=	Net rate of energy gain with flow in and flow out	+	Net rate of energy gain from conduction with tube metal

$$\rho CV_{si}\frac{dT_{si}}{dt} = F_s C_s (T_{si_{in}} - T_{si_{out}}) + hA_{si}(T_{mi} - T_{si}) \qquad (4.2.3)$$

where:

ρ	Water density
C_s	Thermal Capacitance of Subsection
V_{si}	Volume of the i^{th} shell tank
T_{si}	Temperature of the i^{th} shell water tank
T_{mi}	Temperature of the i^{th} tube metal subsection
F_s	Flow rate of the shell side water
$T_{si_{in}}$ $T_{si_{out}}$	Temperature of the input or output water to the i^{th} shell tank
h	Water enthalpy
A_{si}	Heat transfer area for the i^{th} shell tank

Since:

$T_{si_{out}} = T_{si}$ (Average temperature in subsection)

$T_{si_{in}} = T_{s(i-1)}$ (Average temperature in previous subsection)

Equation (4.2.3) becomes:

$$\rho CV_s\frac{dT_{si}}{dt} = F_s C_s (T_{s(i-1)} - T_{si}) + hA_{si}(T_{mi} - T_{si}) \qquad (4.2.4)$$

where:

Volume of subsection	$V_{si} = V_s / N$
Heat Transfer Area for the i^{th} Subsection	$A_{si} = A_s / N$
Thermal Capacitance of Subsection	$C_s = \frac{(\rho CV)_s}{N}$
Flow Resistance on Shell Side	$R_{fs} = \frac{1}{F_s C_s}$
Shell Side to Tube Metal Energy Transfer Resistance	$R_{ms} = \frac{N}{hA_s}$

With these definitions, the i^{th} shell side energy balance becomes

$$C_s \frac{dT_{si}}{dt} = \frac{1}{R_{fs}}(T_{s(i-1)} - T_{si}) + \frac{1}{R_{ms}}(T_{mi} - T_{si}) \tag{4.2.5}$$

and for $i = 1$, $T_{s0} = T_{\sin}$.

For the specific example of dividing heat exchanger into two subsections, the differential equation describing the first and the second shell side subsections are:

$$\frac{dT_{s1}}{dt} = \frac{1}{R_{fs}C_s}(T_{\sin} - T_{s1}) + \frac{1}{R_{ms}C_s}(T_{m1} - T_{s1}) \tag{4.2.6}$$

$$\frac{dT_{s2}}{dt} = \frac{1}{R_{fs}C_s}(T_{s1} - T_{s2}) + \frac{1}{R_{ms}C_s}(T_{m2} - T_{s2}) \tag{4.2.7}$$

4.2.2 Tube Metal Energy Balance for the i^{th} Subsection

The energy balance for the i^{th} shell subsection can be expressed as the following:

Rate of energy storage in subsection	=	Net rate of energy gain from shell side	+	Net rate of energy gain from tube side	+	Net rate of energy gain from neighboring metal subsection

$$C_m \frac{dT_{mi}}{dt} = \frac{1}{R_{ms}}(T_{si} - T_{mi}) + \frac{1}{R_{mt}}(T_{ti} - T_{mi}) + \frac{1}{R_{mm}}\sum_i (T_{mi} - T_{m(i-1)}) \quad (4.2.8)$$

where:

Thermal capacitance of tube metal subsection	$C_m = \frac{(\rho CV)_m}{N}$
Tube side to tube metal energy transfer resistance	$R_{mt} = \frac{N}{h_t A_t}$
Conduction Resistance between metal subsection	$R_{mm} = \frac{L}{kA_m}$

For our case, the energy balance equations for the first and the second tube metal subsections are:

$$\frac{dT_{m1}}{dt} = \frac{1}{R_{ms}C_m}(T_{s1} - T_{m1}) + \frac{1}{R_{mt}C_m}(T_{t1} - T_{m1}) + \frac{1}{R_{mm}C_m}(T_{m2} - T_{m1}) \quad (4.2.9)$$

$$\frac{dT_{m2}}{dt} = \frac{1}{R_{ms}C_m}(T_{s2} - T_{m2}) + \frac{1}{R_{mt}C_m}(T_{t2} - T_{m2}) + \frac{1}{R_{mm}C_m}(T_{m1} - T_{m2}) \quad (4.2.10)$$

4.2.3 Tube Side Energy Balance for the i^{th} Subsection

The energy balance for the i^{th} shell subsection can be expressed as the following:

Rate of energy storage in subsection	=	Net rate of energy gain with flow in and flow out	+	Net rate of energy gain from conduction with tube metal

$$C_t \frac{dT_{ti}}{dt} = \frac{1}{R_{ft}}(T_{t(i+1)} - T_{ti}) + \frac{1}{R_{mt}}(T_{mi} - T_{ti}) \qquad (4.2.11)$$

where

Thermal capacitance of tube side node	$C_t = \frac{(\rho CV)_t}{N}$
Flow resistance on tube side	$R_{ft} = \frac{1}{F_t C_t}$

For the inlet subsection on the tube side, $i = N$ and $T_{t(N+1)} = T_{tin}$ .The differential equations are:

$$\frac{dT_{t1}}{dt} = F_t(T_{t2} - T_{t1}) + \frac{1}{R_{mt}C_t}(T_{m1} - T_{t1}) \qquad (4.2.12)$$

$$\frac{dT_{t2}}{dt} = F_t(T_{tin} - T_{t2}) + \frac{1}{R_{mt}C_t}(T_{m2} - T_{t2}) \qquad (4.2.13)$$

With the relationships described in table 4.4, the mathematical model can be transformed into state-space form.

Table 4.4

Outputs	T_{t2}					
	y					
Inputs	F_S	F_T				
	u_1	u_2				
State Variable	T_{s1}	T_{s2}	T_{m1}	T_{m2}	T_{t1}	T_{t2}
	x_1	x_2	x_3	x_4	x_5	x_6

The derived state-space model is:

$$\dot{x}_1 = F_s(T_{\sin} - x_1) + \frac{1}{R_{ms}C_s}(x_3 - x_1) \tag{4.2.14}$$

$$\dot{x}_2 = F_s(x_1 - x_2) + \frac{1}{R_{ms}C_s}(x_4 - x_2) \tag{4.2.15}$$

$$\dot{x}_3 = \frac{1}{R_{ms}C_m}(x_1 - x_3) + \frac{1}{R_{mt}C_m}(x_5 - x_3) + \frac{1}{R_{mm}C_m}(x_4 - x_3) \tag{4.2.16}$$

$$\dot{x}_4 = \frac{1}{R_{ms}C_m}(x_2 - x_4) + \frac{1}{R_{mt}C_m}(x_6 - x_4) + \frac{1}{R_{mm}C_m}(x_3 - x_4) \tag{4.2.17}$$

$$\dot{x}_5 = F_t(x_6 - x_5) + \frac{1}{R_{mt}C_t}(x_3 - x_5) \tag{4.2.18}$$

$$\dot{x}_6 = F_t(T_{tin} - x_6) + \frac{1}{R_{mt}C_t}(x_4 - x_6) \tag{4.2.19}$$

$$y = T_{t2} \tag{4.2.20}$$

4.3 Target Tank Modeling

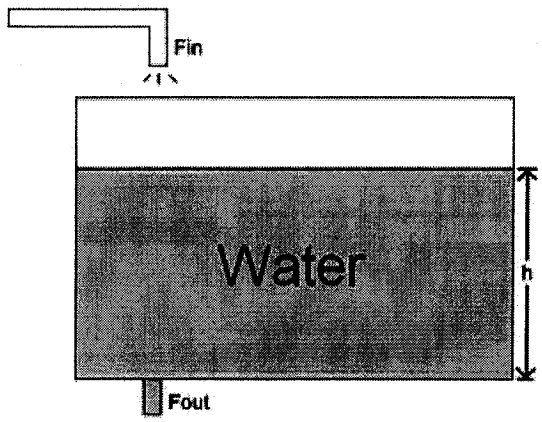

Figure 4.5

Figure 4.5 is a graph showing the target tank to be modeled. On top of the tank, there is a hose adding water into the tank at a flow rate of *Fin*. This flow rate can be adjusted by the servo valve located in the primary water circulation. At the same time, water in the tank is leaking out from an orifice located in the bottom of the water tank. This flow rate is *Fout*. A change in the inlet water's flow rate can adjust the tank's water level *h*.

The mathematical equation describing this water tank is:

$$A\frac{dh}{dt} = F_{In} - F_{Out} \tag{4.3.1}$$

where A is the cross section of the water tank.

From Torricelli's principle, F_{out} can be calculated as:

$$F_{out} = a\sqrt{2gh} \tag{4.3.2}$$

where a is the cross section area of the orifice and g is the gravitational acceleration constant.

By plugging (4.3.2) into (4.3.1), we obtain the following nonlinear model:

$$\frac{dh}{dt} = \frac{F_{IN}}{A} - \frac{a\sqrt{2gh}}{A} \tag{4.3.3}$$

Define the following variables for this water tank system model:

State Variable	h
	x
Input	F_{IN}
	u

The system model then becomes:

$$\dot{x} = -\frac{a\sqrt{2g}}{A}\sqrt{x} + \frac{1}{A}u \tag{4.3.4}$$

At this point, models for the water tank and the heat exchanger have been obtained.

4.4 Linearization of Nonlinear Mathematical Models

4.4.1 Linearization of the Target Tank Model

A system is nonlinear if the principle of superposition does not apply. Thus, for a nonlinear system the response to two inputs cannot be calculated by treating one input at a time and adding the results. The derived models from the previous sections of this chapter are all nonlinear models. To further the analysis and study of the plant using linear tools, we now linearize all of these models.

In control engineering, normal operation of the system may be around some operating point, and the signals may be considered small signal deviations around the operating point. If all these requirements are met, then it is possible to approximate the nonlinear system by a linear system. Such a linear system is almost equivalent to the nonlinear system considered within a limited operating range.

Assume we have a time-invariant nonlinear model with n states, m inputs and p outputs:

$$\begin{aligned} \dot{x} &= f(x,u) \\ y &= h(x,u) \end{aligned} \tag{4.4.1}$$

For constant $u = u^*$, x^* is an equilibrium state if $f(x^*,u^*) = 0$. This means if $x = x^*$ and $u = u^*$, then $\dot{x} = 0$ and the state remains at x^*, i.e., x^* is an equilibrium point with $u = u^*$. The output corresponding to an equilibrium state $x = x^*$ is $y^* = h(x^*,u^*)$.

The next step is to write equations for incremental variables, i.e., for deviations from equilibrium. Let

$$\begin{aligned} x(t) &= x^* + \Delta x(t) \\ u(t) &= u^* + \Delta u(t) \\ y(t) &= y^* + \Delta y(t) \end{aligned}$$

Since $\dot{x}^* = 0$, substituting the above into equation 4.4.1 yields:

$$\begin{aligned} \Delta\dot{x} &= f(x^* + \Delta x, u^* + \Delta u) \\ \Delta y &= h(x^* + \Delta x(t), u^* + \Delta u) - y^* \end{aligned} \tag{4.4.2}$$

Expanding the components of f in a Taylor series, we obtain

$$\begin{aligned} f_i(x^* + \Delta x, u^* + \Delta u) &= f_i(x^*, u^*) + \frac{\partial f_i}{\partial x_1}\Big|_* \Delta x_1 + \frac{\partial f_i}{\partial x_2}\Big|_* \Delta x_2 + \cdots \\ &+ \frac{\partial f_i}{\partial x_m}\Big|_* \Delta x_n + \frac{\partial f_i}{\partial u_1}\Big|_* \Delta u_1 + \cdots + \frac{\partial f_i}{\partial u_r}\Big|_* \Delta u_r + \text{higher-order terms in } \Delta x, \Delta u. \end{aligned} \tag{4.4.3}$$

In Equation (4.4.3), the notation "$|_*$" means "evaluated at (x^*, u^*)." At this point, it is assumed that Δx and Δu are sufficiently small to justify neglecting the higher-order terms. Since $f(x^*, u^*) = 0$, the RHS of (4.4.3) is the i^{th} member of a set of n equations, written in matrix form as

$$f(x^* + \Delta x, u^* + \Delta u) = \frac{\partial f}{\partial x}\Big|_* \Delta x + \frac{\partial f}{\partial u}\Big|_* \Delta u \tag{4.4.4}$$

where

$$\frac{\partial f}{\partial x} = \begin{bmatrix} \frac{\partial f_1}{\partial x_1} & \cdots & \frac{\partial f_1}{\partial x_n} \\ \vdots & \ddots & \vdots \\ \frac{\partial f_n}{\partial x_1} & \cdots & \frac{\partial f_n}{\partial x_n} \end{bmatrix} \tag{4.4.5}$$

is the Jacobian of f with respect to the state x, with a similar definition for $\frac{\partial f}{\partial u}$, the Jacobian with respect to the input u. Thus, equation 4.4.2 becomes approximately

$$\begin{aligned} \Delta\dot{x} &= \frac{\partial f}{\partial x}\Big|_* \Delta x + \frac{\partial f}{\partial u}\Big|_* \Delta u \\ \Delta y &= \frac{\partial h}{\partial x}\Big|_* \Delta x + \frac{\partial h}{\partial u}\Big|_* \Delta u \end{aligned} \tag{4.4.6}$$

In our case, the equilibrium operating point was chosen to be such that the target tank is about half full. (This equilibrium operating point is thought of as a feedback-controlled equilibrium.) Numerically:

$$h_e = 0.05m$$

The associated equilibrium flow rate for the above level can be calculated from (4.3.4).

Recall the nonlinear model derived for the target tank is:

$$\dot{x} = -\frac{a\sqrt{2g}}{A}\sqrt{x} + \frac{1}{A}u \tag{4.4.7}$$

Applying linearization method to the model, the linearized model should take the form of

$$\Delta\dot{x}(t) = \frac{\partial f}{\partial x}\Delta x(t) + \frac{\partial f}{\partial u}\Delta u(t) \tag{4.4.8}$$

where:

$$\frac{\partial f}{\partial x} = \frac{-a\sqrt{2g}}{2\sqrt{h_e}A}, \qquad \frac{\partial f}{\partial u} = \frac{1}{A}$$

4.4.2 Linearization of the Heat Exchanger Models

Recall the nonlinear model derived from the first modeling approach:

$$\dot{x}_1 = u_1(A_3T_{C0} - A_3x_1) - (A_1x_1 - A_1x_4) \tag{4.4.9}$$
$$\dot{x}_2 = u_1(A_3x_1 - A_3x_2) - (A_1x_2 - A_1x_3) \tag{4.4.10}$$
$$\dot{x}_3 = u_2(A_4T_{H0} - A_4x_3) - (A_2x_3 - A_2x_2) \tag{4.4.11}$$
$$\dot{x}_4 = u_2(A_4x_3 - A_4x_4) - (A_2x_4 - A_2x_1) \tag{4.4.12}$$

The operation point for u_1 is already calculated in the previous section to be $0.003\ m^3/\min$. For the second input's operation point, it is set to be $0.00047\ m^3/\min$, which is a half of the secondary circulation's maximum flow rate. Applying the linearization method, the linearized model will take the form:

$$\begin{aligned} \Delta\dot{x} &= A\Delta x + B\Delta u \\ \Delta y &= C\Delta x + D\Delta u \end{aligned} \tag{4.4.13}$$

where

$$A = \begin{bmatrix} \frac{\partial f_1}{\partial x_1} & \cdots & \frac{\partial f_1}{\partial x_4} \\ \vdots & & \vdots \\ \frac{\partial f_4}{\partial x_1} & \cdots & \frac{\partial f_4}{\partial x_4} \end{bmatrix} = \begin{bmatrix} (-u_1A_3 - A_1) & 0 & 0 & A_1 \\ u_1A_3 & (-u_1A_3 - A_1) & A_1 & 0 \\ 0 & A_2 & (-u_2A_4 - A_2) & 0 \\ A_2 & 0 & u_2A_4 & (-u_2A_4 - A_2) \end{bmatrix} \tag{4.4.14}$$

$$B = \begin{bmatrix} \frac{\partial f_1}{\partial u_1} & \frac{\partial f_1}{\partial u_2} \\ \vdots & \vdots \\ \frac{\partial f_4}{\partial u_1} & \frac{\partial f_4}{\partial u_2} \end{bmatrix} = \begin{bmatrix} A_3T_{C0} - A_3x_1 & 0 \\ A_3x_1 - A_3x_2 & 0 \\ 0 & A_4T_{h0} - A_4x_3 \\ 0 & A_4x_3 - A_4x_4 \end{bmatrix} \tag{4.4.15}$$

$$C = \begin{bmatrix} \frac{\partial g_1}{\partial x_1} & \cdots & \frac{\partial g_1}{\partial x_4} \end{bmatrix} = \begin{bmatrix} 0 & 1 & 0 & 0 \end{bmatrix} \tag{4.4.16}$$

$$D = 0 \tag{4.4.17}$$

With the equilibrium values and parameters, matrices A and B become:

$$A=\begin{bmatrix} \frac{\partial f_1}{\partial x_1} & \cdots & \frac{\partial f_1}{\partial x_4} \\ \vdots & & \vdots \\ \frac{\partial f_4}{\partial x_1} & \cdots & \frac{\partial f_4}{\partial x_4} \end{bmatrix}=\begin{bmatrix} -2.3041 & 0 & 0 & 0.3153 \\ 1.9889 & -2.3041 & 0.3153 & 0 \\ 0 & 0.3503 & -0.5105 & 0 \\ 0.3503 & 0 & 0.1598 & -0.5105 \end{bmatrix} \tag{4.4.18}$$

$$B=\begin{bmatrix} \frac{\partial f_1}{\partial u_1} & \frac{\partial f_1}{\partial u_2} \\ \vdots & \vdots \\ \frac{\partial f_4}{\partial u_1} & \frac{\partial f_4}{\partial u_2} \end{bmatrix}=\begin{bmatrix} -22160 & 0 \\ -61060 & 0 \\ 0 & 430120 \\ 0 & -156120 \end{bmatrix} \tag{4.4.19}$$

The controllability matrix of this derived model has a rank of 4 which indicates the model is fully controllable. Several open loop simulations on this linearized model have been done through a Matlab program. Experimental data records showed that the simulation done with this system model could simulate the real heat exchanger very well.

Linearization for the mathematical model derived from the second approach has been done in the same way from the method applied on the first one. The linearized model takes the form of:

$$\begin{aligned} \dot{x}_1 &= u_1(T_{\text{sin}} - x_1) + A_1(x_3 - x_1) \\ \dot{x}_2 &= u_1(x_1 - x_2) + A_1(x_4 - x_2) \\ \dot{x}_3 &= A_2(x_1 - x_3) + A_3(x_5 - x_3) + A_4(x_4 - x_3) \\ \dot{x}_4 &= A_2(x_2 - x_4) + A_3(x_6 - x_4) + A_4(x_3 - x_4) \\ \dot{x}_5 &= u_2(x_6 - x_5) + A_5(x_3 - x_5) \\ \dot{x}_6 &= u_2(T_{\text{tin}} - x_6) + A_5(x_4 - x_6) \end{aligned} \tag{4.4.20}$$

where:

$$A_1 = \frac{1}{R_{ms} \cdot C_s},\quad A_2 = \frac{1}{R_{ms} \cdot C_m}$$

$$A_3 = \frac{1}{R_{mt} \cdot C_m},\quad A_2 = \frac{1}{R_{mm} \cdot C_m},\quad A_5 = \frac{1}{R_{mt} \cdot C_t}$$

Another Matlab program has been created to test the performance of this model. However, experiments showed that the second model's step response is not as

good as that of the first model. The decision of using the first derived model is made for the sake of applying a mathematical model that has a better performance in simulating the real physical system.

4.5 Summary

The reason why the first model has better simulation results is that in this modeling approach, the tube metal was overlooked while the second model took the tube metal into consideration. Since the heat exchanger used is only 15cm in length and the tube metal's thickness is only 1mm, the heat conducting process in the tube metal is of very little significance. Ignoring the heat transfer process in the tube metal, we obtained a model that simulated the exchanger's dynamics better. However, if the heat exchanger utilized were a large scale one, the second model approach may have had a more acceptable simulation performance. Putting the linearized models together, we have the following mathematical model representing the real plant.

$$\begin{bmatrix} \dot{x}_1 \\ \dot{x}_2 \\ \dot{x}_3 \\ \dot{x}_4 \\ \dot{x}_5 \end{bmatrix} = \begin{bmatrix} -2.3041 & 0 & 0 & 0.3153 & 0 \\ 1.9889 & -2.3041 & 0.3153 & 0 & 0 \\ 0 & 0.3503 & -0.5105 & 0 & 0 \\ 0.3503 & 0 & 0.1598 & -0.5105 & 0 \\ 0 & 0 & 0 & 0 & -3.3181 \end{bmatrix} \begin{bmatrix} x_1 \\ x_2 \\ x_3 \\ x_4 \\ x_5 \end{bmatrix} + \begin{bmatrix} -22160 & 0 \\ -61060 & 0 \\ 0 & 430120 \\ 0 & -156120 \\ 52.102 & 0 \end{bmatrix} \begin{bmatrix} u_1 \\ u_2 \end{bmatrix}$$

$$\begin{bmatrix} y_1 \\ y_2 \end{bmatrix} = \begin{bmatrix} 0 & 1 & 0 & 0 & 0 \\ 0 & 0 & 0 & 0 & 1 \end{bmatrix} \begin{bmatrix} x_1 \\ x_2 \\ x_3 \\ x_4 \\ x_5 \end{bmatrix}$$

where:

State Variables		Inputs		Outputs	
$x_1 \cdots x_4$	Heat Exchanger Subsection's Average Temperature	u_1	Primary Circulation Flow Rate	y_1	Target Tank Water Temperature
x_5	Water Level	u_2	Secondary Circulation Flow Rate	y_2	Target Tank Water Level

Chapter 5 Multivariable Decoupling Control Design

Recall the complete model derived:

$$\begin{bmatrix}\dot{x}_1\\ \dot{x}_2\\ \dot{x}_3\\ \dot{x}_4\\ \dot{x}_5\end{bmatrix} = \begin{bmatrix}-2.3041 & 0 & 0 & 0.3153 & 0\\ 1.9889 & -2.3041 & 0.3153 & 0 & 0\\ 0 & 0.3503 & -0.5105 & 0 & 0\\ 0.3503 & 0 & 0.1598 & -0.5105 & 0\\ 0 & 0 & 0 & 0 & -3.3181\end{bmatrix}\begin{bmatrix}x_1\\ x_2\\ x_3\\ x_4\\ x_5\end{bmatrix} + \begin{bmatrix}-22160 & 0\\ -61060 & 0\\ 0 & 430120\\ 0 & -156120\\ 52.102 & 0\end{bmatrix}\begin{bmatrix}u_1\\ u_2\end{bmatrix}$$

$$\begin{bmatrix}y_1\\ y_2\end{bmatrix} = \begin{bmatrix}0 & 1 & 0 & 0 & 0\\ 0 & 0 & 0 & 0 & 1\end{bmatrix}\begin{bmatrix}x_1\\ x_2\\ x_3\\ x_4\\ x_5\end{bmatrix}$$

In this MIMO system, there are two inputs and two outputs. The two inputs are the flow rates of the primary and secondary water circulations. The outputs are the temperature and level of water in the *Target Tank*.

To control the plant, we have attempted three decoupling control schemes. Due to the system model's limitation, only one is applicable to the system under study. Nevertheless, we present all the methods in this chapter because the abandoned methods may still shed some light on other decoupling control system design problems.

5.1 Multivariable Decoupling Control with Decoupling Network

In an MIMO system, there is interaction among the inputs and the outputs. In most cases, designing non-interacting control schemes can alleviate this interaction. The goal is to eliminate the coupling effects between control loops. This is achieved by the specification of compensation networks known as *decouplers*. The following diagram shows the general construction of a Decoupling Control System with decoupler.

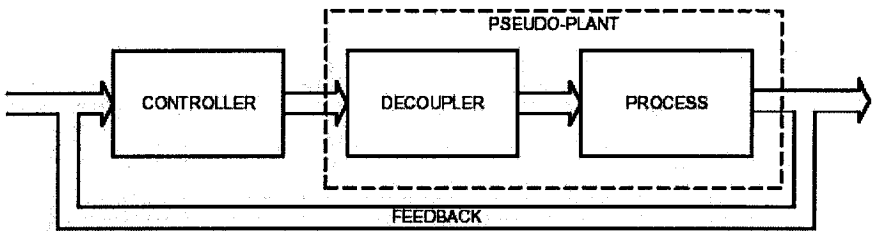

Figure 5.1 Decoupling Control System with Decoupler

The role of the decoupler is to decompose a multivariable process into a series of independent single-loop sub-systems. If such a situation can be achieved, then complete or ideal decoupling occurs and the multivariable process can be controlled using independent SISO loop controllers.

Figure 5.2 shows the scheme of Decoupling Control with Decoupling Network

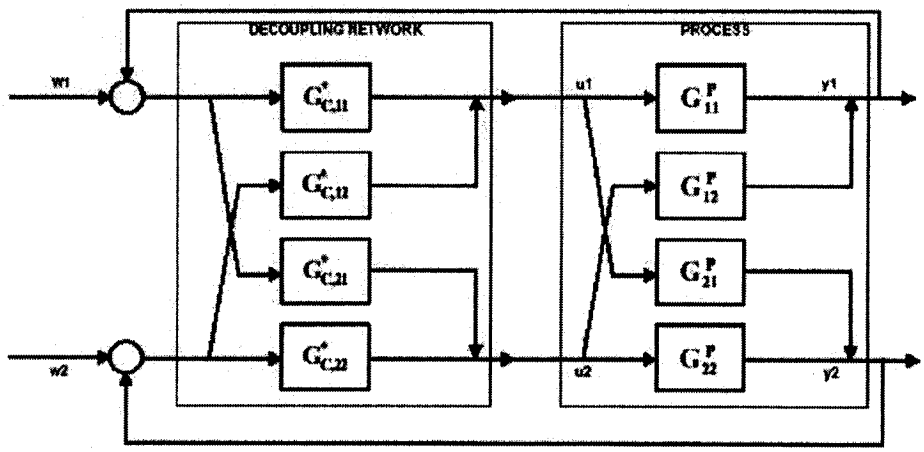

Figure 5.2 Decoupling Control Scheme

In this method, let G_c^* be the matrix of decoupling elements:

$$G_C^* = \begin{pmatrix} G_{C,11}^* & G_{C,12}^* \\ G_{C,21}^* & G_{C,22}^* \end{pmatrix} \tag{5.1.1}$$

and let the system model be represented in the P-canonical form:

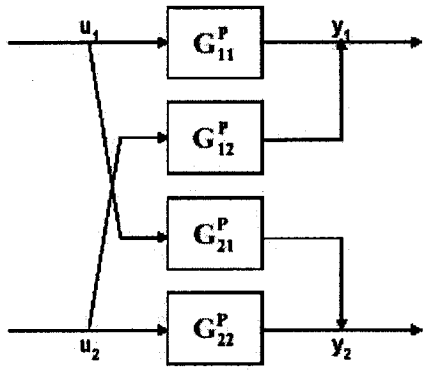

$$\begin{aligned} y_1 &= G_{11}^P u_1 + G_{12}^P u_2 \\ y_2 &= G_{12}^P u_1 + G_{22}^P u_2 \end{aligned} \tag{5.1.2}$$

Introducing a vector of reference signals, $w = [w_1, w_2]^T$ results in the following equations:

$$\begin{aligned} &Gu = y \text{ with } u = G_C^*[w - y] \\ &\Rightarrow GG_C^*[w - y] = y \end{aligned} \tag{5.1.3}$$

Rearrangement of the above yields the closed loop expression:

$$y = [I + G \cdot G_C^*]^{-1} GG_C^* w \tag{5.1.4}$$

For the individual loops of the closed loop system to be independent of one another, it is required that:

$$T = [I + G \cdot G_C^*]^{-1} GG_C^* = diag(t_1, t_2) \tag{5.1.5}$$

i.e. T must be a diagonal matrix.

Since the sum and product of two diagonal matrices are diagonal matrices, and the inverse of a diagonal matrix is also a diagonal matrix, then the requirement can be ensured if $G \cdot G_c^*$ is made diagonal, i.e.

$$GG_C^* = \begin{pmatrix} G_{11} & G_{12} \\ G_{21} & G_{22} \end{pmatrix}\begin{pmatrix} G_{C,11}^* & G_{C,12}^* \\ G_{C,21}^* & G_{C,22}^* \end{pmatrix} = \begin{pmatrix} q_1 & 0 \\ 0 & q_2 \end{pmatrix}$$
$$\Rightarrow \begin{pmatrix} G_{11}G_{C,11}^* + G_{12}G_{C,21}^* & G_{11}G_{C,12}^* + G_{12}G_{C,22}^* \\ G_{21}G_{C,11}^* + G_{22}G_{C,21}^* & G_{21}G_{C,12}^* + G_{22}G_{C,22}^* \end{pmatrix} = \begin{pmatrix} q_1 & 0 \\ 0 & q_2 \end{pmatrix} \quad (5.1.6)$$

Comparing each element of the matrices results in a set of four equations:

$$\begin{aligned} q_1 &= G_{11}G_{C,11}^* + G_{12}G_{C,21}^* \\ 0 &= G_{11}G_{C,12}^* + G_{12}G_{C,22}^* \\ 0 &= G_{21}G_{C,11}^* + G_{22}G_{C,21}^* \\ q_1 &= G_{21}G_{C,12}^* + G_{22}G_{C,22}^* \end{aligned} \quad (5.1.7)$$

Since the transfer function elements of G are known, and we can specified the diagonal elements of G_c^*, then the appropriate off-diagonal elements of G_c^* to achieve decoupling control can be calculated by solving the above set of equations. The simplest way to do this is to concentrate on the conditions that will set GG_c^* to a diagonal matrix, i.e. the above equations whose left-hand side zero. These give the following relationships:

$$G_{C,12}^* = \frac{-G_{12}G_{C,22}^*}{G_{11}} \quad \text{and} \quad G_{C,21}^* = \frac{-G_{21}G_{C,11}^*}{G_{22}} \quad (5.1.8)$$

If the forward path decoupling elements, $G_{C,11}^*$ and $G_{C,22}^*$ are taken to be PID controllers, then given the transfer functions of the process, the decoupling network will be fully specified. The limitation of this method is that $G_{C,12}^*$ and $G_{C,21}^*$ are dependent on $G_{C,11}^*$ and $G_{C,22}^*$. This means if any of the forward path compensation elements are tuned on-line, the off-diagonal compensation elements must be recalculated. This makes the applicability of this control scheme more difficult. Due to this reason, some modification has been made to avoid the inconvenience encountered.

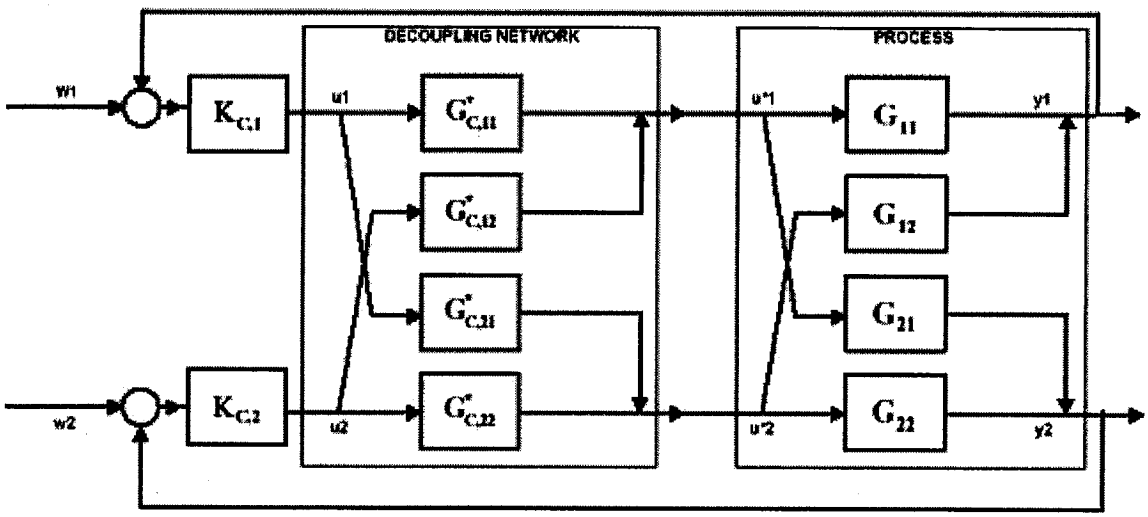

Figure 5.3 Revised Decoupling Control Scheme

Here, in addition to the decoupling network, there are two extra blocks, which represent the forward path controllers. In contrast to the previous strategy, the decoupling network forms the secondary post-compensation block and allows more flexibility in the implementation of the non-interacting control scheme. Let the forward path control matrix be denoted K_C with output u, and the output of the decoupling network be denoted u^*. The system can be described by the following relationships:

$$\begin{aligned} & y = Gu^* \\ & u^* = G_C^* u \qquad \Rightarrow y = GG_C^* \cdot u = GG_C^* K[w-y] \\ & u = K[w-y] \end{aligned} \tag{5.1.9}$$

Our objective here is to create a situation where the forward path controllers 'think' that they are controlling two independent loops. The objective will be achieved if:

$$H = GG_C^* = diag[q_1.q_2] \tag{5.1.10}$$

To determine G_c^*, we have to calculate the inverse of G.

Since:

$$G_C^* = G^{-1}H \text{ with } G^{-1} = adj(G)/\det(G) \tag{5.1.11}$$

where $adj(G)$ and $\det(G)$ denote the *adjoint* and the *determinant* of the matrix G respectively, and they are given by:

$$\det(G) = G_{11}G_{22} - G_{12}G_{21} \tag{5.1.12}$$

$$adj(G) = \begin{bmatrix} G_{22} & -G_{12} \\ -G_{21} & G_{11} \end{bmatrix} \tag{5.1.13}$$

Since $H = diag\begin{bmatrix} q_1 & q_2 \end{bmatrix}$, therefore

$$G_C^* = G^{-1}H = \begin{bmatrix} G_{22}q_1 & -G_{12}q_2 \\ -G_{21}q_1 & G_{11}q_2 \end{bmatrix} \frac{1}{\det(G)} \tag{5.1.14}$$

The simplest form of this decoupling matrix has unity diagonal elements, which means: $G_{C,11}^* = G_{C,22}^* = 1$ i.e. $q_1 = \frac{1}{G_{22}}$ and $q_2 = \frac{1}{G_{11}}$.

This leads to the following off-diagonal elements:

$$G_{C,12}^* = -G_{12}/G_{11} \quad and \quad G_{C,21}^* = -G_{21}/G_{22}$$

For the system under study, G_{22} is calculated to be 0. This makes it impossible to calculate $G_{C,21}^*$. This problem happens in the application of both presented methods. Nevertheless, we have tried to perturb slightly the system model so it can be suitable for this decoupling control scheme. What I have done is changing the order of the two sub-models in the complete plant model. This leads to the following state-space system:

$$\begin{bmatrix} \dot{x}_1 \\ \dot{x}_2 \\ \dot{x}_3 \\ \dot{x}_4 \\ \dot{x}_5 \end{bmatrix} = \begin{bmatrix} 0 & 0 & 0 & 0 & -3.3181 \\ -2.3041 & 0 & 0 & 0.3153 & 0 \\ 1.9889 & -2.3041 & 0.3153 & 0 & 0 \\ 0 & 0.3503 & -0.5101 & 0 & 0 \\ 0.3503 & 0 & 0.1598 & -0.5101 & 0 \end{bmatrix} \begin{bmatrix} x_1 \\ x_2 \\ x_3 \\ x_4 \\ x_5 \end{bmatrix} + \begin{bmatrix} 52.102 & 0 \\ -22160 & 0 \\ -61060 & 0 \\ 0 & 430120 \\ 0 & -156120 \end{bmatrix} \begin{bmatrix} u_1 \\ u_2 \end{bmatrix}$$

$$\begin{bmatrix} y_1 \\ y_2 \end{bmatrix} = \begin{bmatrix} 1 & 0 & 0 & 0 & 0 \\ 0 & 0 & 1 & 0 & 0 \end{bmatrix} \begin{bmatrix} x_1 \\ x_2 \\ x_3 \\ x_4 \\ x_5 \end{bmatrix}$$

But after a further examine of the model, we realized that this system is highly unstable. At this point, we gave up the efforts of trying to apply the system model

with the decoupling network method, and turned to the relative gain array technique instead.

5.2 Relative Gain Decoupling

Another approach to deal with control loop interaction is to find a proper choice of input-output pairings such that the interactions will be minimized.

An "*nxn*" system will give rise to "n!" possible Input-Output pairings. N control loops will be applied after we have found out what pairing scheme should be used in the system. It is important to be able to evaluate quantitatively, the degree of interaction between the control loops of the system. This information can then be used as a guide to structure a minimal interaction control scheme. The *Relative Gain Array (RGA)* analysis technique is one such methodology.

For an MIMO system with matrix transfer function $G_0(s)$, the RGA is defined as a matrix λ with the ij^{th} element:

$$\lambda_{ij} = [G_0(0)]_{ij}[G_0^{-1}(0)]_{ji} \qquad (5.2.1)$$

where $[G_0(0)]_{ij}$ denotes the ij^{th} element of the plant dc gain matrix and $[G_0^{-1}(0)]_{ji}$ denotes the ji^{th} element of the inverse of the plant dc gain matrix, respectively.

In (5.2.1), $[G_0(0)]_{ij}$ corresponds to the dc gain from the j^{th} input u_j to the i^{th} output y_i, while the other inputs are kept constant. Also, $[G_0^{-1}(0)]_{ji}$ is the reciprocal of the d.c. gain from the j^{th} input u_j to the i^{th} output y_i, while the other outputs are kept constant. Hence, the parameter λ_{ij} indicates how sensible it is to pair the j^{th} input u_j to the i^{th} output y_i.

In our case, the calculated RGA is:

$$\lambda=\begin{pmatrix}0 & 1\\ 1 & 0\end{pmatrix}$$

Since the RGA derived has zero valued diagonal elements and unity off-diagonal elements, this indicates that control of the system can be achieved by pairing y_1 with u_2 and y_2 with u_1.

Actually, this result is very compatible with the real experiment equipment. Recall that "u_1" and "u_2" represent the primary and secondary water flow rate while " y_1 " and " y_2 " represent the target tank's water temperature and level, respectively. The water level is solely controlled by the primary water circulation and has nothing to do with the secondary water flow rate.

5.3 Simulation

The following Simulink model has been created to test the feasibility of using the RGA pairing method.

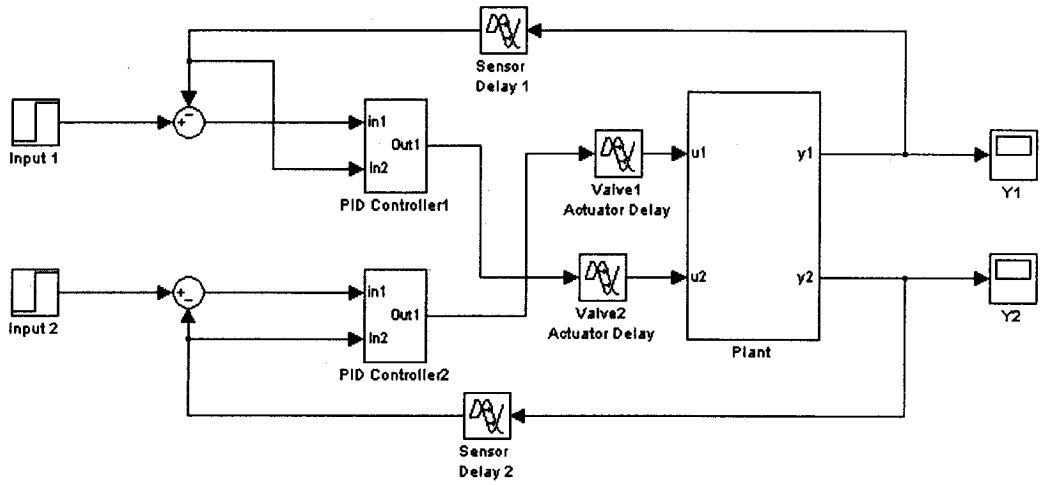

Figure 5.4 Simulink Model using RGA pairing method

The controllers applied in the model are of PID type. They are shown in figure 5.5.

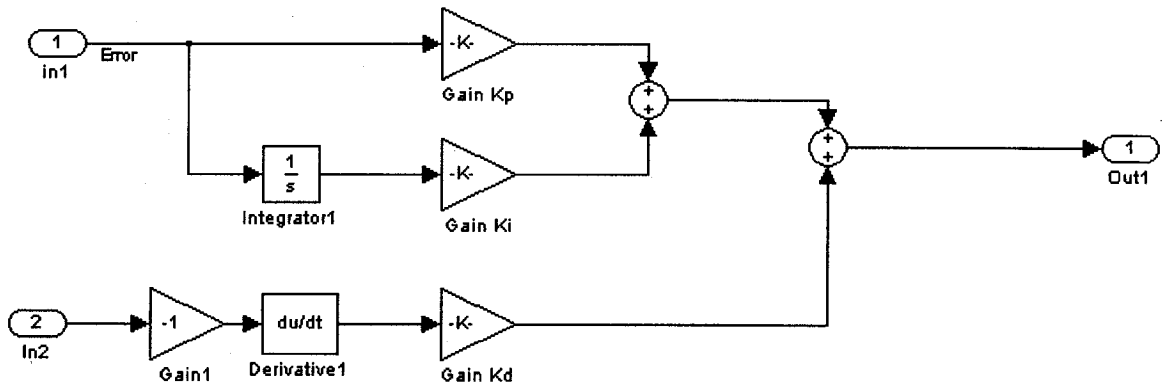

Figure 5.5 PID Controller used to Control the Plant

The following plots illustrate some of the simulation results from this Simulink Model. The control signals are within their saturation limits.

For the first simulation, the temperature input is 35 and the level input is 10.

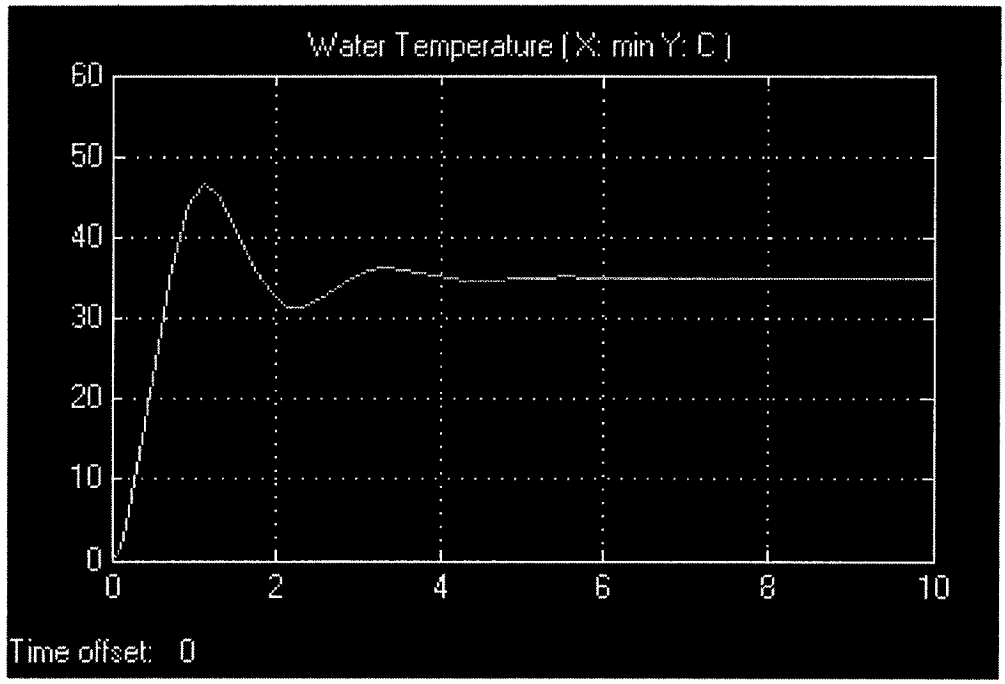

Figure 5.6 First Simulation Result (Water Temperature)

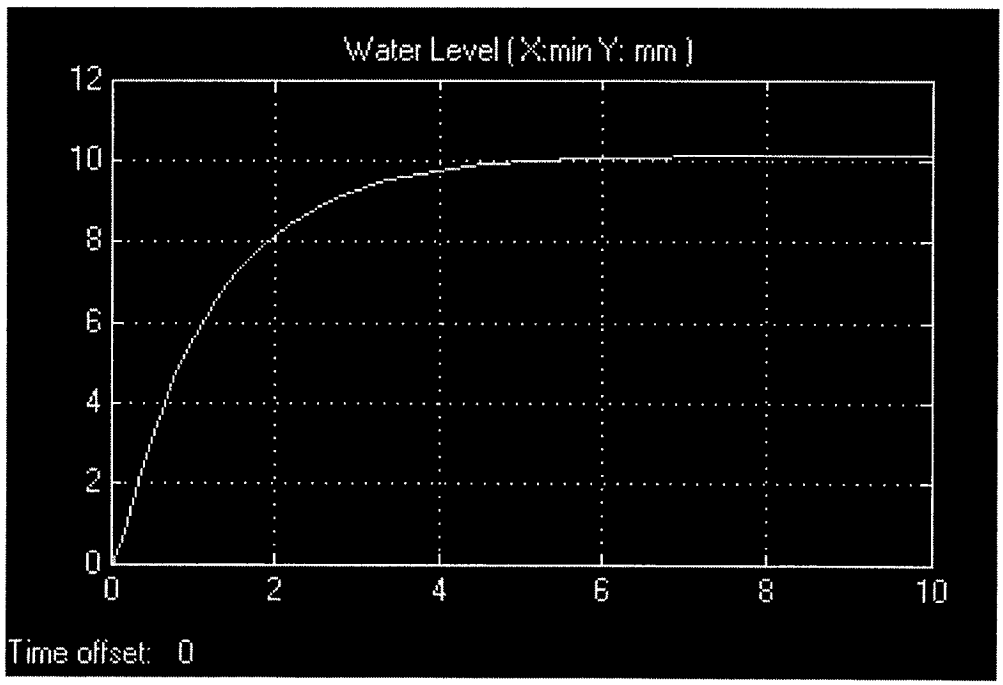

Figure 5.7 First Simulation Result (Water Level)

The second simulation's input temperature is 10 and the level input is 50.

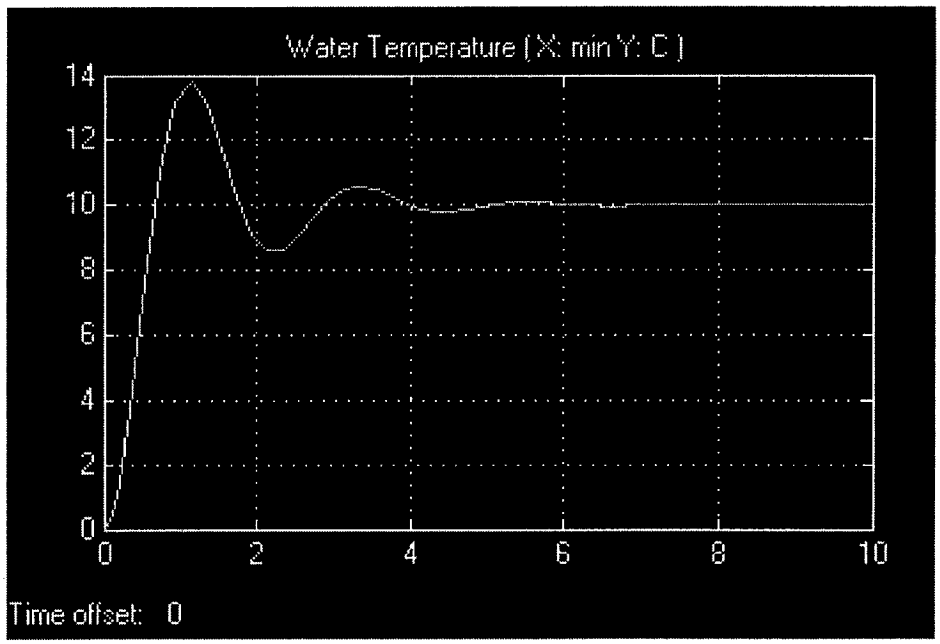

Figure 5.8 Second Simulation Result (Water Temperature)

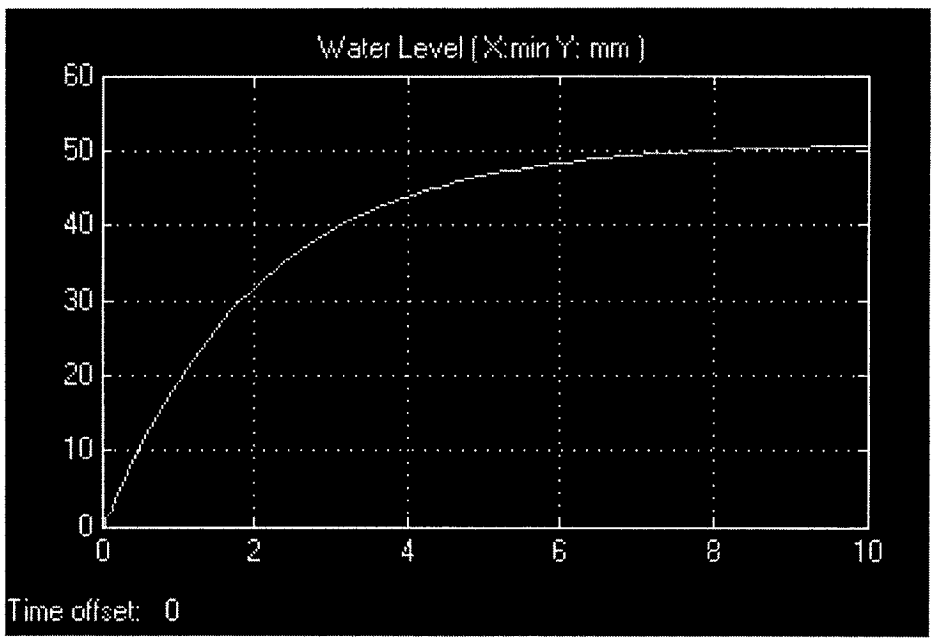

Figure 5.9 Second Simulation Result (Water Level)

The above simulation results show that the best pairing indicated by the RGA method can be applied to the model under study with good results. Further control system design is then based on this decoupling approach.

Chapter 6 Control System Configuration

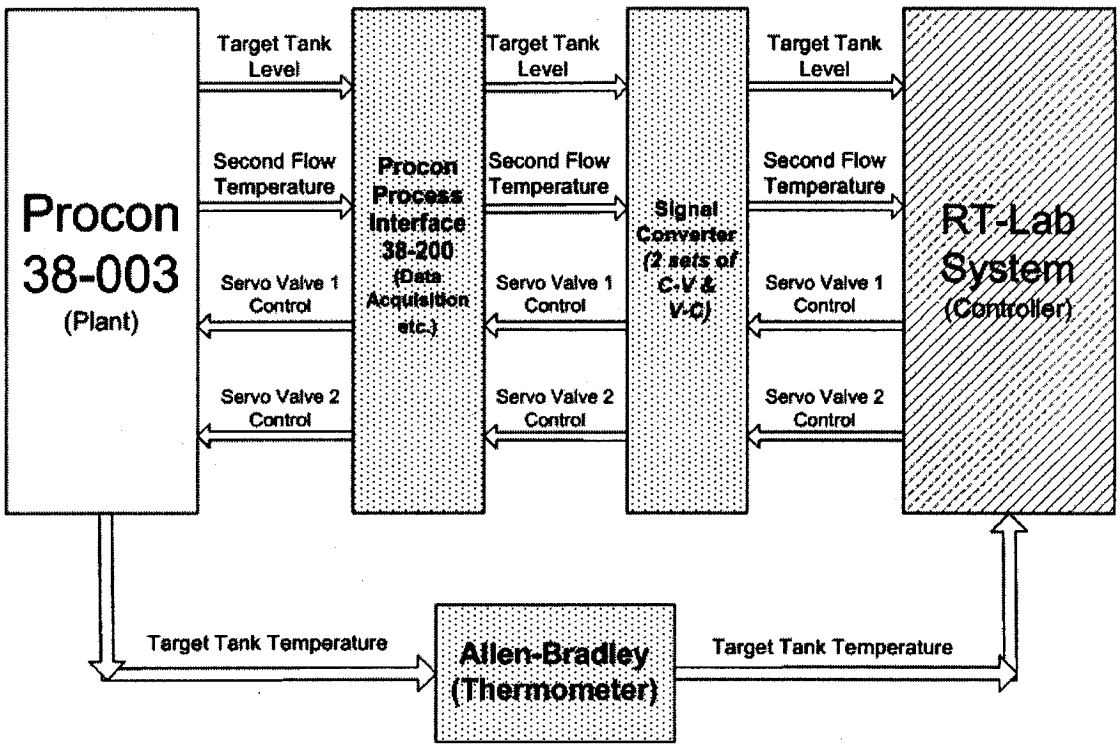

Figure 6.1 Control System Configuration

Figure 6.1 illustrates the configuration of the whole control system setup. The system can be divided into three main sections. This chapter will present a detailed description for each of the section in the above control system.

6.1 Procon 38-003

The first section of the whole control system is the Procon 38-003. Please refer to the third chapter of this thesis for a thorough explanation on this equipment. One thing to note here is that there are three sensors mounted in the Procon 38-003. They are for the measurement of *Target Tank Level (TTL)*, *Target Tank Temperature (TTT)* and *Second Flow Temperature (SFT).*

6.2 Signal Processing Unit

The dotted blocks in figure 6.1 represent the devices in the second section of the system. These devices are the *Procon Process Interface 38-200*, the *Signal Converters* and the *Allen-Bradley 1746 Open Controller.*

6.2.1 Procon Process Interface 38-200

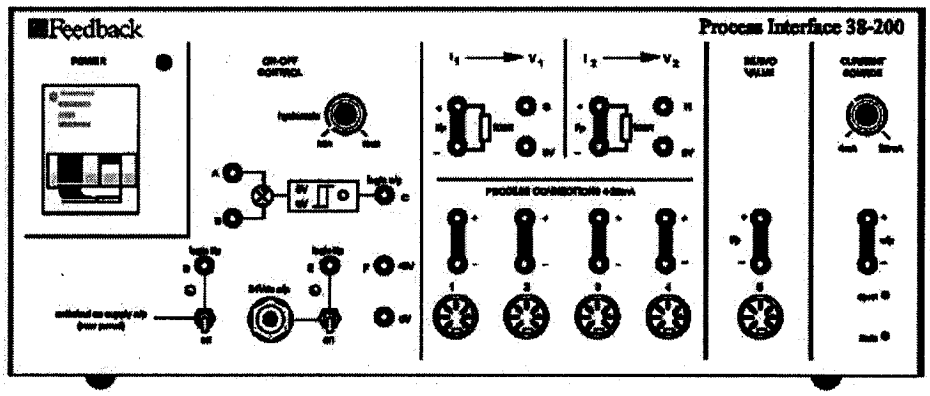

Figure 6.2 Process Interface 38-200

The Procon 38-200 serves as the data acquisition unit for the parameters measured by the *TTL* and *SFT* sensors. It also provides power for each of the devices installed in the Procon 38-003. This device accepts four sensor signal inputs and one servo valve signal output. Since the Procon 38-200 only supports 4-20mA current signals while the I/O board (NI 6036E) used in RT-Lab Target Node machine only works with Voltage signals (-10V-10V), two types of signal converters have been built to make the equipment operate seamlessly.

6.2.2 Signal Converters

6.2.2.1 Voltage–to-Current Converter

In an ideal voltage-to-current (V/I) converter, an input voltage modulates the power from the power supply and yields an output current that tracks the input voltage, without any distortion in amplitude or phase. Very little energy is transferred from the signal source to the converter. [13]

V/I converters (-10~10V to 4~20mA) can be implemented by a handful of resistors and active components. The functions required for the converter are scaling V/I conversion and offsetting (-10V to 4mA), which can be performed in any order. Figure 6.3 shows the designed and implemented circuit for the V/I converter.

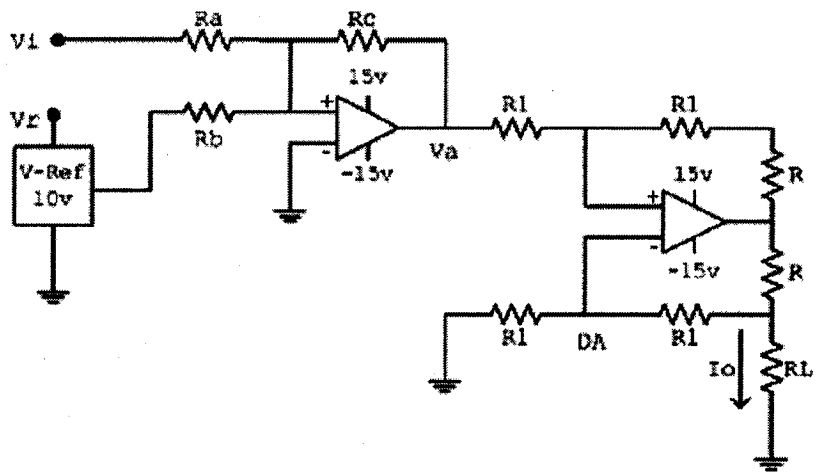

Figure 6.3 Voltage-Current Signal Converter Circuit

In this circuit, first a constant voltage is added and then the resulting voltage is converted to a current using a single-ended V/I converter. The op amp output voltage is

$$v_a = -v_i \frac{R_c}{R_a} - v_r \frac{R_c}{R_b} \tag{6.2.1}$$

and

$$I_o = -v_a \frac{R_1 + R}{R_1 R} \tag{6.2.2}$$

Hence:

$$I_o = \left(\frac{V_i}{R_a} + \frac{V_r}{R_b}\right) \frac{R_c (R_1 + R)}{R_1 R} \tag{6.2.3}$$

By selecting R1=100 kΩ, R=100Ω Rc=1kΩ and Vr=10V and plugging these parameters into equation (6.2.3), we have:

when *Vi=-10V,*

$$0.004 = (\frac{-10}{R_a} + \frac{10}{R_b}) \frac{1000 \times (100 \times 10^3 + 100)}{100 \times 10^3 \times 100} \tag{6.2.4}$$

when *Vi=10V,*

$$0.02 = (\frac{10}{R_a} + \frac{10}{R_b}) \frac{1000 \times (100 \times 10^3 + 100)}{100 \times 10^3 \times 100} \tag{6.2.5}$$

Solving (6.2.4) and (6.2.5), we have the result of Ra=12.5kΩ and Rb=8.3kΩ. Table 6.1 summarizes the electronic components used in the V/I Converter.

Table 6.1

Component	Specification	Number
R_a	12.5kΩ	1
R_b	8.3kΩ	1
R_c	1kΩ	1
R	100Ω	2
R_1	100 kΩ	4
OP-Amp	OP27	2

The performance of this converter is shown in figure 6.4.

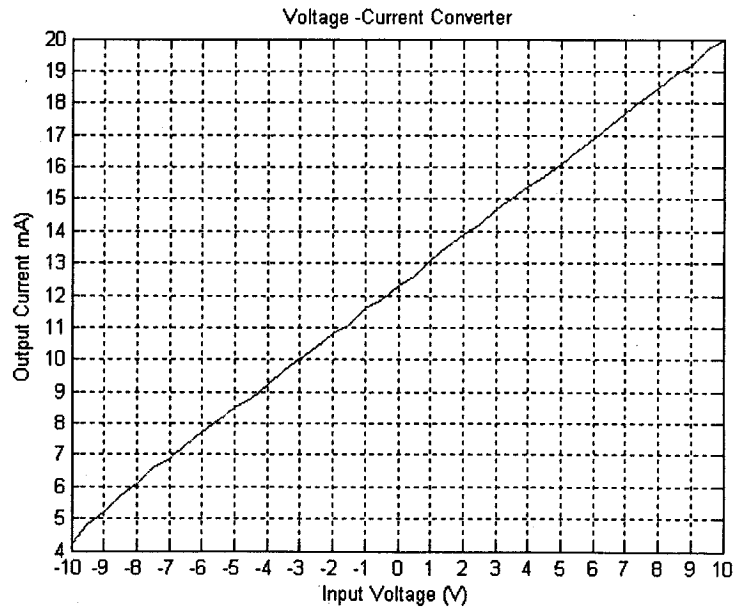

Figure 6.4 Voltage-Current Signal Converter Circuit Performance

6.2.2.2 Current–to-Voltage Converter

Similar to the V/I converter, in an ideal current-to-voltage converter, an input current signal modulates power from the power supply and provides an output voltage that tracks the input current, ideally without any distortion in amplitude or phase. Very little energy is transferred from the signal source to the next stage.

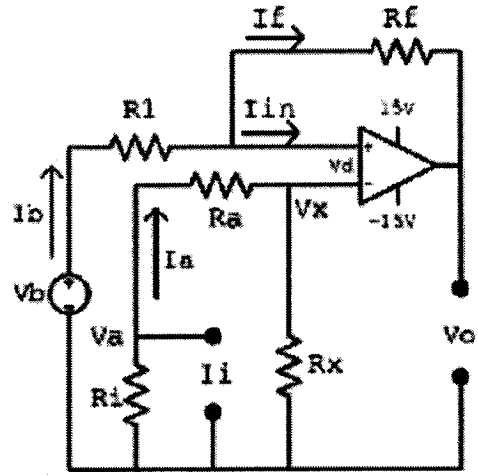

Figure 6.5 Current-to-Voltage Signal Converter Circuit

'Va' in figure 6.5 is created by the input current signal *'Ii'*. Since the input current signal *'Ii'* is in the range of 4~20mA, I have added this current signal on a resistor *'Ri'* which is 1kΩ. I am quite awarded that using such method to generate a voltage source in the circuit is not so ideal. But after the circuit is built, the performance of this converter is very satisfactory. Since the emphasis of this thesis' research is not about the circuit design, I have accepted this circuit even though it is not the perfect design.

In figure 6.5 *Vx* can be related to the input voltage *Va* by

$$V_x = \frac{R_x}{R_x + R_a} V_a \tag{6.2.6}$$

The output voltage *Voa* which is due to the input at the Op-Amp's non-inverting terminal is:

$$V_{oa} = (1+\frac{R_f}{R_1})V_x = (1+\frac{R_f}{R_1})\frac{R_x}{R_x+R_a}V_a \tag{6.2.7}$$

The output voltage *Vob* which is due to the input at the Op-Amp's inverting terminal is

$$V_{ob} = -\frac{R_f}{R_1}V_b \tag{6.2.8}$$

Therefore, the resulting output voltage is given by

$$V_o = V_{ob} + V_{oa} = -\frac{R_f}{R_1}V_b + (1+\frac{R_f}{R_1})\frac{R_x}{R_x+R_a}V_a \tag{6.2.9}$$

By selecting $R_i = R_a = R_1 = R_x = 1K\Omega$ and $R_f = 4K\Omega$, the circuit can linearly convert 4~20mA input into -10~10V output.

The following graph shows the performance of this converter.

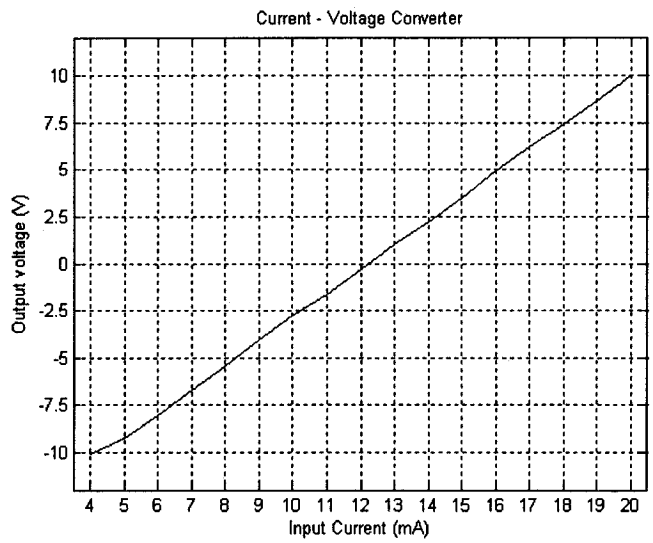

Figure 6.6 Current-Voltage Signal Converter Circuit Performance.

6.2.3 Thermocouple/mV Input Module and UNAC Model

With the integration of the Procon 38-200 and the signal converters, parameters like *TTL* and *SFT* can be measured while the control system is working. At the same time, the *Thermocouple/mV Input Module* installed in the Allen-Bradley 1747 OC measures *Target Tank Temperature (TTT)* in real time.

The *thermocouple/mV input module* receives and stores digitally converted thermocouple and/or millivolt (mV) analog data into its image table for retrieval by all fixed and modular SLC500 processors. The module contains a removable terminal block with two cold junction compensation (CJC) sensors. There are no output channels on the module. Configuration and monitoring of this module is done via the UNAC control software package. The following figure shows the UNAC model working with the thermocouple/mV input module.

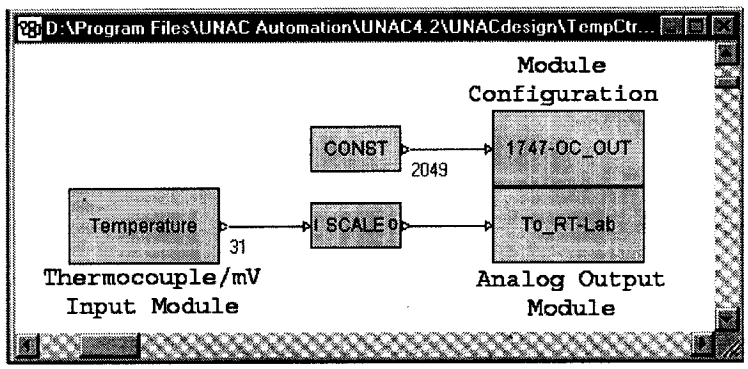

Figure 6.6 UNAC model

In the UNAC model, the *const* block serves for configuring the *Thermocouple/mV Input Module*. Once the module is installed, each channel on the module must be configured to establish the way the channel will operate. This is done by entering bit values into the configuration word using the software. The value 2049 is chosen such that the Thermocouple Input Module is configured to use the metric system and the measured temperature values are expressed in increments of 0.1 degree Celsius, etc.

The UNAC model's Temperature block monitors the Target Tank Temperature taken by the Thermocouple Input Module. The measured values are sent to the Analog Output Module which outputs a voltage signal on the Analog Output Module of the AB 1747. A *scale* block is added to linearly transform the temperature values into voltage values which range from -10V to 10V.

6.3 RT-Lab Workstation

The third section of the control system is the RT-Lab workstation.

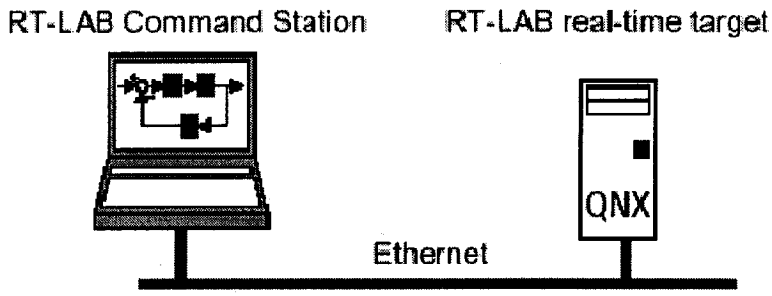

Figure 6.7 RT-Lab workstation

RT-Lab is used as the controller part of the whole control system. The above figure shows the configuration of the RT-Lab system.

Users interact with RT-Lab during a simulation by using the *Command Station*, a work station operating under Windows NT. Communication between the *Command Station* and the *Target Node* is performed through a TCP/IP connection. This allows users to save any signal from the model, for viewing or for off-line analysis. It is also possible to use the *Command Station* to modify the model's parameters while the simulation is running.

In the *Target Node*, there is an I/O board mounted. With this I/O device, the *Target Node* can take the signal transmitted by the signal converter and then feed it into the RT-Lab model, which is running simultaneously in both the *Target Node* and *Command Station*. RT-Lab then analyzes the data and generates control signals for the process. (These are voltage signals and are needed to be transformed into current signals by V/I converters.) A more detailed description of RT-Lab System can be found in the following chapter.

6.4 Summary

When the control system is working, three parameters are constantly being measured from the plant. These are *Target Tank Level (TTL), Target Tank Temperature (TTT) and Second Flow Temperature (SFT).* The *TTL* and *SFT* signals are transmitted by the Feedback Interface 38-200 and transferred into voltage signals by I/V converters. At the same time, the *TTT* signal is measured by the thermocouple input module installed in AB 1747 and is fed into RT-Lab system.

Control Signals generated by RT-Lab pass through the converters and go into the Feedback Interface 38-200. The servo valves in Procon 38-003 take these control signals to set their openings to achieve the goal of adjusting the flow rate in both the primary and secondary circulations.

Chapter 7 RT-Lab System and Model

The RT-Lab workstation serves as the software configurable controller for devices in the Industrial Automation Laboratory. The author has prepared a manual for this system. The document can be found at the following URL:

http://www.cim.mcgill.ca/%7Eialab/members/usefuldoc/RT-Lab_Instructions_v1.pdf

Since presenting a detailed explanation of the RT-Lab system is impossible in this thesis, only a brief description of the system configuration and how RT-Lab works will be stated in this chapter.

7.1 RT-Lab System Configuration

RT-Lab runs on a hardware configuration consisting of a Command Station, a Target Node, Communication Links (real-time and Ethernet), and I/O boards.

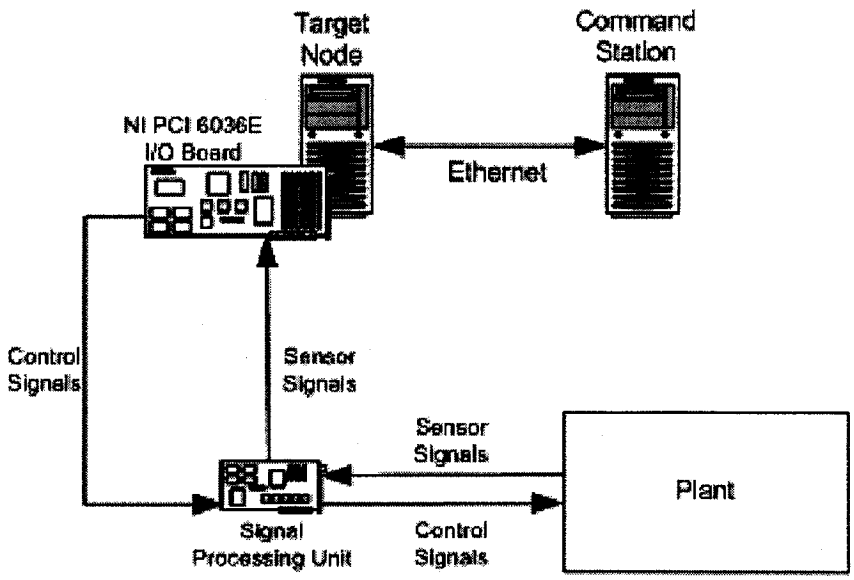

Figure 7.1 RT-Lab System Configuration

RT-Lab Command Station is used as the host and user interface. It allows users to:

- Edit and modify models;
- Monitor model behavior in real-time;
- Run the original model under its simulation software (Simulink, etc.);
- Control the simulator's Go/Stop sequences.

The RT-Lab Target Node is a commercial PC, equipped with PC-compatible processors, which operates in a QNX environment. In the QNX environment, the real-time sending and reception of data between QNX nodes is typically performed through FireWire-type communication boards.

The real-time Target Node performs:

- Real-time execution of the model's simulation;
- Real-time communication between the nodes and I/Os;
- Initialization of the I/O systems;
- Acquisition of the model's internal variables and external outputs through I/O modules;

The RT-LAB software is an industrial-grade package for engineers who use mathematical block diagrams for simulation, control, and related applications. The software is layered on top of industry-proven, commercial-off-the-shelf (COTS) components like popular diagramming tools MATLAB/Simulink and works with viewers such as LabVIEW and programming languages including Visual Basic and C++.

Once the built Simulink model is validated, the user separates it into subsystems and inserts appropriate communication blocks *OpComm*. Each subsystem will be executed by a *Target Node* in RT-LAB's distributed system.

RT-LAB can automatically distribute its calculations among the Target Nodes, and provides an interface so users can execute the simulation and manipulate the RT-Lab model's parameters. The result is high-performance simulation that can run in parallel and in real-time.

The RT-Lab system in McGill University's Industrial Automation Lab uses an I/O device installed in *Target Node* to communicate with other experiment devices. The I/O device utilized is a National Instruments PCI 6036E data acquisition board shown in Figure 7.2.

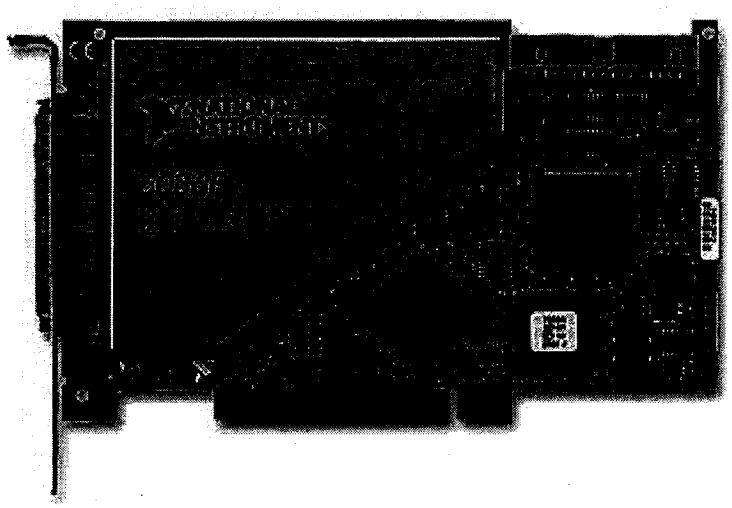

Figure 7.2 NI PCI 6036E

This board has 16 analog inputs (AI), 2 analog outputs (AO) and 8 digital I/O channels (DI, DO). The following table illustrates the channels used in our RT-Lab Model.

Channel	Specification	Comment
AO 1	Control Signal for Servo Valve 1	
AO 2	Control Signal for Servo Valve 2	
AI 1	Target Tank Temperature	From AB 1747 Open Controller
AI 2	Target Tank Level	From Procon 38-200
AI 3	Second Flow Temperature	From Procon 38-200
DO 1	Primary Pump Control	
DO 2	Secondary Pump Control	
DO 3	Heater Control	
DO 4	Target Tank Solenoid Switch Control	

7.2 RT-Lab Model

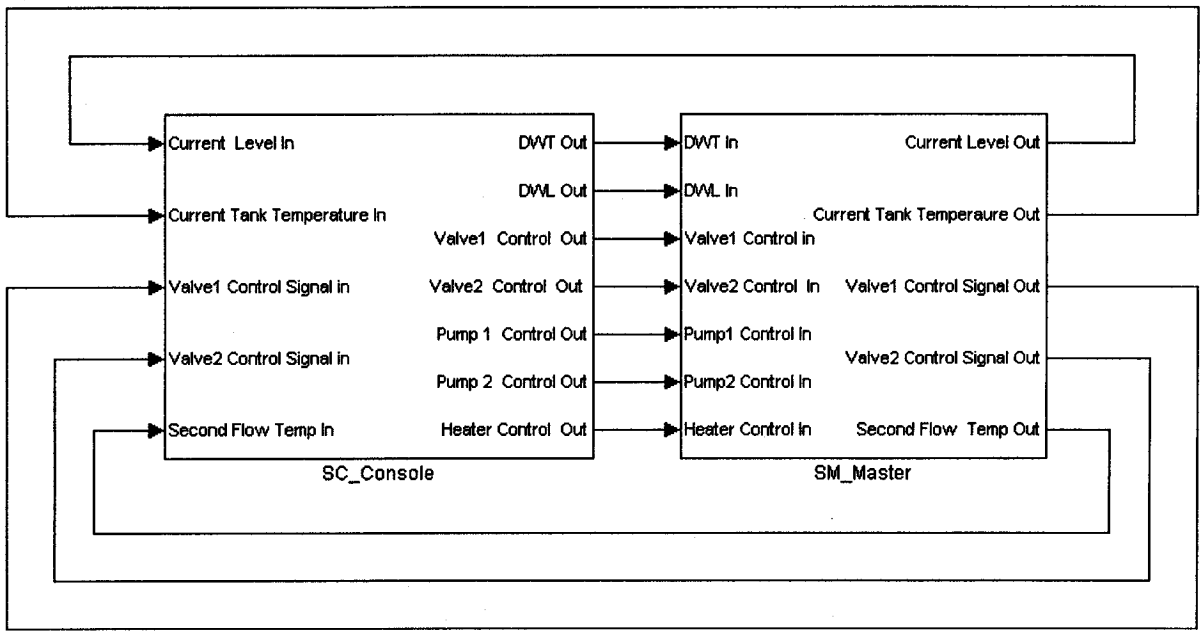

Figure 7.3 RT-Lab Model

In the above model, each of the two blocks represents a subsystem. These two subsystems are distributed into RT-Lab's workstations and ran simultaneously.

7.2.1 *SC_Console* subsystem

SC_Console subsystem at the left of figure 7.3 runs in RT-Lab's *Command Station*, where the user interacts with the simulation process. It contains all the Simulink blocks related to acquiring and viewing data (scope, manual switch, etc.). The structure of this subsystem is illustrated in Figure 7.4.

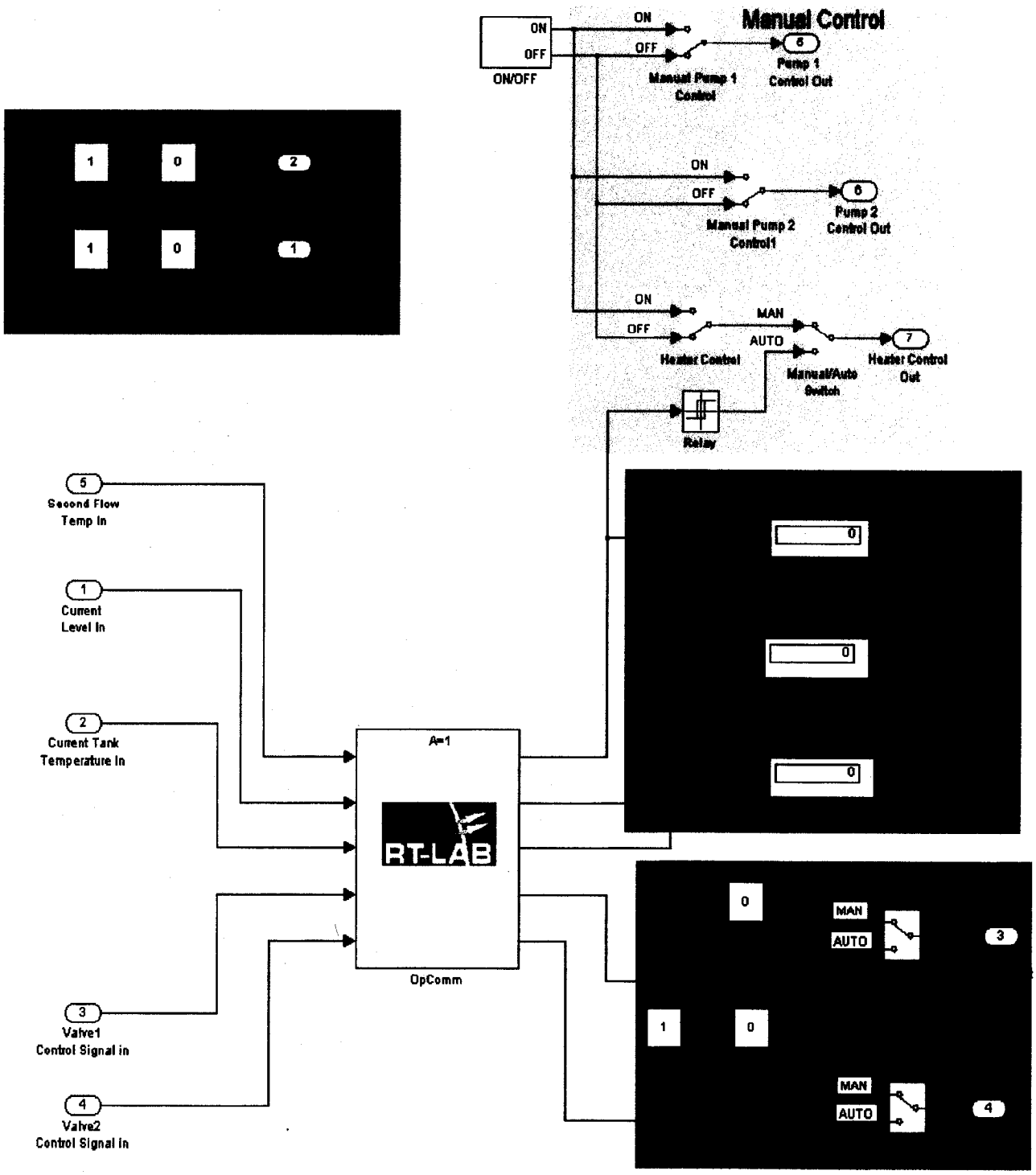

Figure 7.4 SC_Console Subsystem

In the top left area of the *SM_Master* subsystem in the figure, the user can define the desired target tank water temperature and level through the *Slide Gain* blocks. These user inputs are sent to the controller in *SM_Master* subsystem running in *Target Node*. (A more detailed description of *SM_Master* subsystem will be presented later in this chapter.).

To the right of the *User Input* section are the *Manual Control* blocks of this model. These blocks allow the user to control the primary and the secondary pumps' ON/OFF status.

The *Heater Control* in this section has two modes, Auto and Manual. In manual mode, the user can switch the secondary circulation heater On or Off at his/her own wish. When working in Auto mode, the *Relay* block in this section sets the heater on when the secondary water flow is lower than 55 degree and off when the water temperature goes over 56. This enables the water flows into the heat exchanger to remain close to a constant temperature.

The *Display* section of this subsystem has three *Display* blocks. They are for showing the parameters of *Second Flow Temperature*, *Target Tank Temperature* and *Target Tank Level* in real time.

SC_Console's *Valve Control* section enables the user to control Servo Valves either manually or automatically. In manual mode, user can adjust the opening of the servo valves by the two *Slide Gain* blocks. When the switches are set to "Auto", the control signals from the controller in *SM_Master* are used to operate the valves and the *Slide Gain* blocks become ineffective to control the system.

The *OpComm* block in the middle of this model is a feed-through block required by RT-Lab system. This block serves the following purposes:

1. When a simulation model runs in the RT-Lab environment, all connections between the subsystems are replaced by hardware communication links.

2. OpComm block provides information to RT-Lab concerning the type and size of the signals being sent from one subsystem to another.

7.2.2 *SM_Master* Subsystem

As it is described in the previous paragraphs, *SC_Console* subsystem contains all the blocks that are needed for user interaction. The *SM_Master* model, however, is responsible for the model's real-time calculations and for the overall synchronization of the network. It includes blocks that represent operations to be performed on signals. This subsystem structure is shown in the diagram of Figure 7.5.

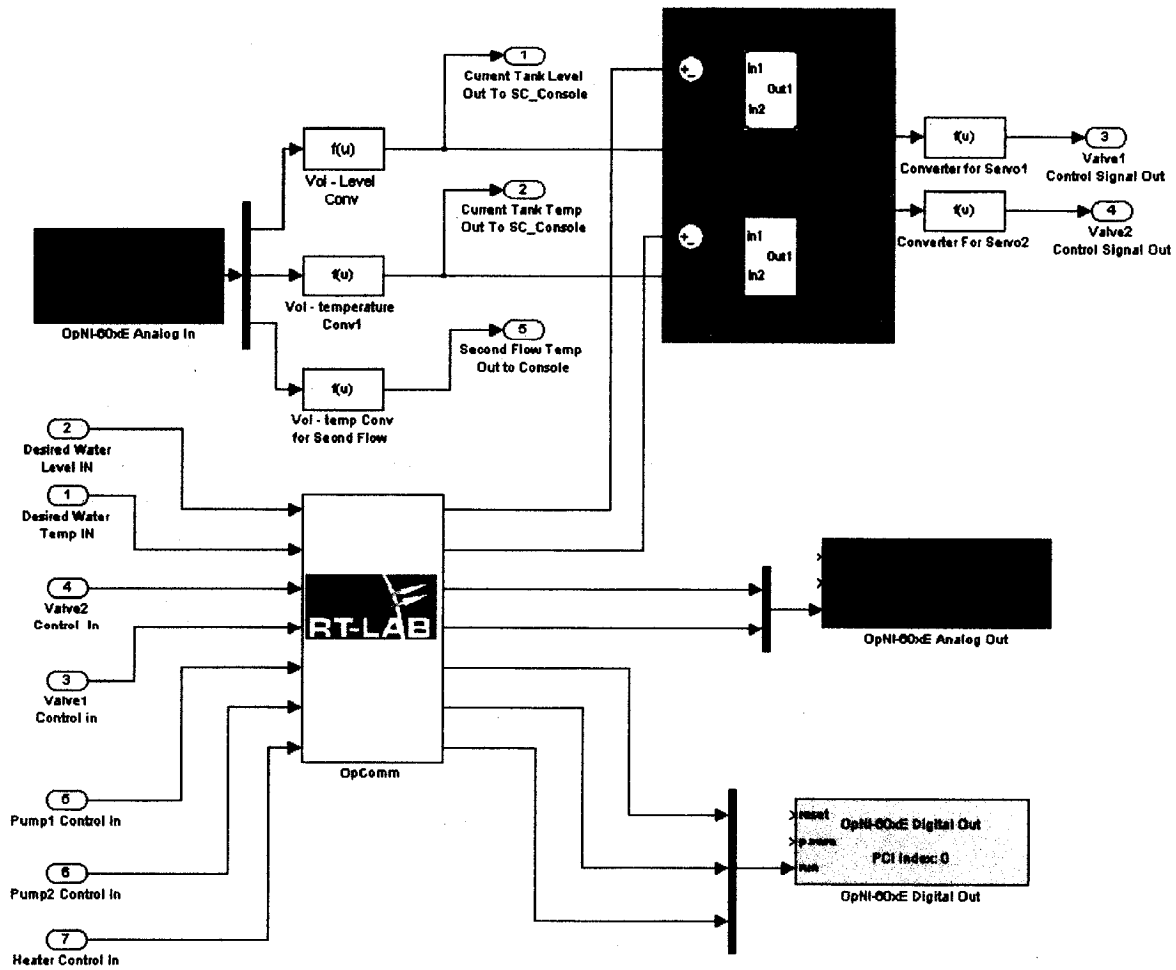

Figure 7.5 SM_Master Subsystem

At the top of this subsystem is the *OpNI-60xE Analog In* block, which takes the signals *TTL*, *TTT* and *SFT* into the RT-Lab model. Three converters are added to transform the signal voltage values back to their original units which can be used in the RT-Lab model. These blocks contain linear functions to serve this purpose.

The converted *TTL* and *TTT* signals are sent to be processed by the controller directly. The applied controllers are both of PID type as shown in Figure 5.5. Tuning of the controller parameters was based on Ziegler-Nichols rules ([10]

Ogata) using the simulation model and finely tuning of this controller is based on actual experiments.

The Control signals sent by the controllers are transformed into voltage values and sent to *SC_Console*'s *valve control* section. If the switch of this section is set at "AUTO", these control signals will be sent back to *SM_Master*'s *OpNI-60xE Analog Out* block, which sends the control signals to the I/O board's designated AO channels.

The *OpNI-60xE Digital Out* block in this subsystem sends the control signals to the I/O Board's DO channels. These signals are from *SC_Console*'s *Manual Control* section.

As the reader may have noticed, putting all SC_Console subsystem's I/O blocks (*OpNI-60xE Analog In, Analog Out and Digital Out*) into SM_Master can largely simplify the model structure. However, this is violating to the rules of building a RT-Lab model. RT-Lab system requires all I/O blocks to be put in a subsystem running in the Target Node, where the I/O board is mounted. (Please note that SC_Console subsystem is running in the target node machine in which I/O board NI6036E is mounted)

7.3 Control System Performances

To demonstrate the performance of the designed control system, the results of two experiments are listed in this section. A discussion on these results will be presented at the end of this section.

For the first experiment, the input temperature was 60 Celsius Degree and the input water level was 60mm. The following plots exhibit the experimental results obtained with the user setpoints. These results can be compared, at least qualitatively to the simulation results of Figures 5.6~5.9.

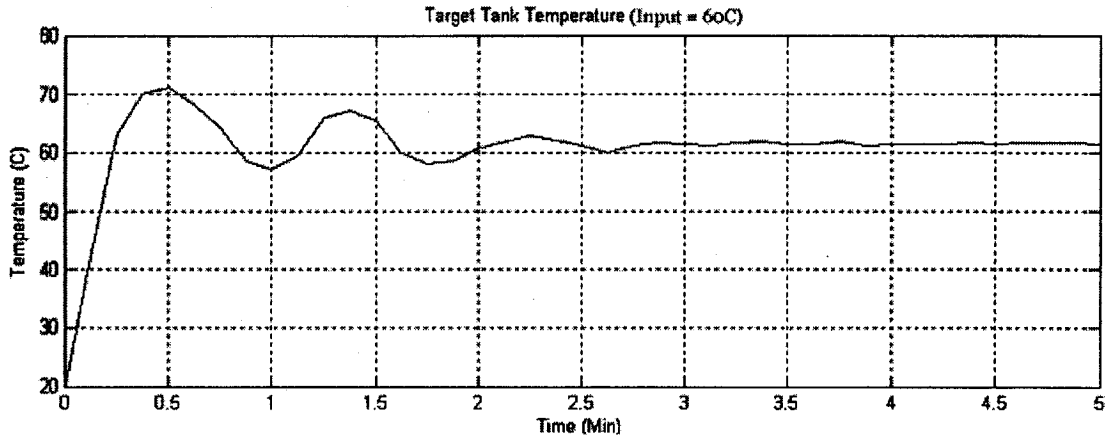

Figure 7.6 First Experiment Result (Water Temperature)

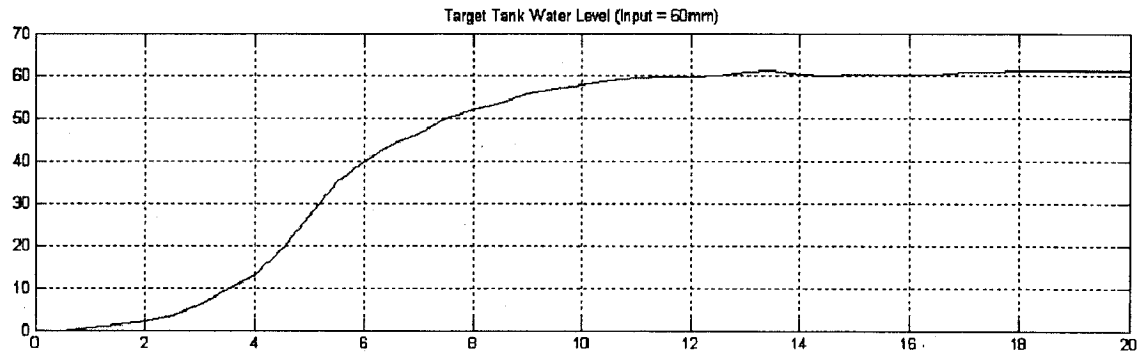

Figure 7.7 First Experiment Result (Water Level)

For the second experiment, the temperature is 35 Celsius Degree and the desired water level is 100 mm.

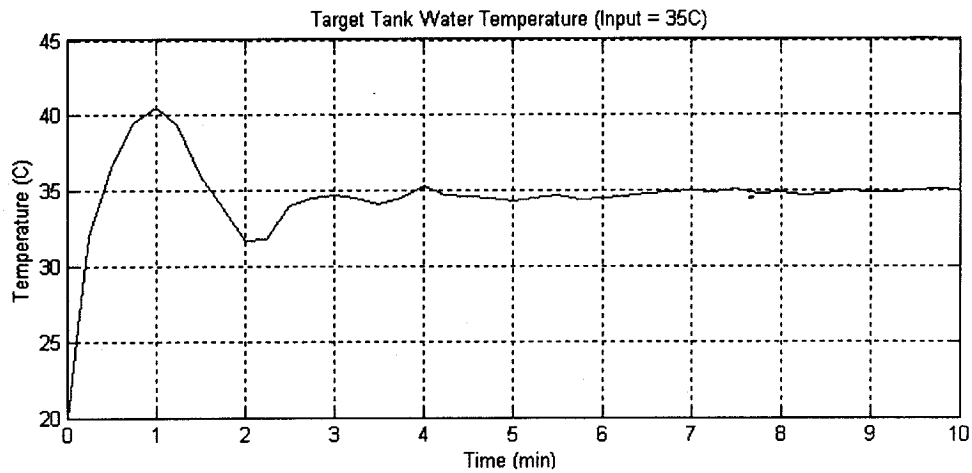

Figure 7.8 Second Experiment Result (Water Temperature)

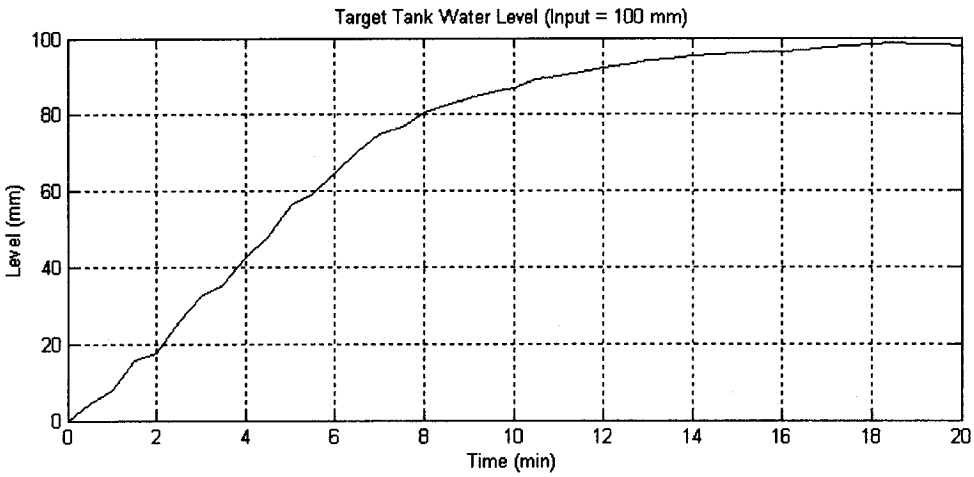

Figure 7.9 Second Experiment Result (Water Level)

Chapter 8 Discussion and Conclusion

As it is shown in previous chapter's experiment results, the target tank's water temperature and level can achieve the desired input status and keeps at a steady state. This shows the designed control system is applicable and desirable.

For the water temperature control, the overshoot is fairly large, on the order of 25%, but this was expected as a similar overshoot was present in the simulated response. This phenomenon may be caused by two reasons. The first possible cause of this problem is the servo valve's response delay. The second possible cause of the overshoot is the heat exchanger. When the water in the second flow is being heated up from room temperature to the working temperature, the secondary circulation is non-stop. This makes the primary water remaining in the exchanger to be warmed up to a rather high temperature. The overshoot may probably be alleviated if the secondary flow could be stopped when the heating process is in progress. However, Procon 38-200 does not have any more free channels to allow this to be done.

For the water level control, the rise time is seen to be fairly long and the response exhibits a very small overshoot. This is due to the primary pump's efficiency. The *Target Tank*'s input current is not high enough to achieve a flow rate that is high enough to compensate the water leaking out of this tank from the orifice in the bottom. This problem may be solved by applying a water pump which can provide a higher flow rate for the primary circulation. However, a change of this pump will result in a change in the plant model. Whether this solution is applicable will remain unknown until a new plant model is created and analyzed.

Also, the working range of the control system is:

Target Tank Water Level (Approximate Value): 0 ~ 100 (mm)

Target Tank Water Temperature (Approximate Value): 26 ~ 60 (Celsius Degree)

When user inputs are out of these ranges, the control system may not give a very good control operation.

This is due to the limitation on the linearization method applied on the derived model. The linearization is based on the operation point of the system under study. When the user inputs have too big a difference from the system operation points, the behavior and dynamics of the linearized model and original model will become dissimilar. This leads to the incapability of the designed system in controlling the variables of interest.

In addition, the steady states in the experimental records occasionally have a slight difference from the desired input level. This variation is caused by several reasons. One of theses causes is the signal transfer process. The sensor-measured signals have to go through a series of devices before they are fed into the controller model. The same situation happens to the control signals. This procedure may give rise to the steady-state error. Eliminating or alleviating this error may be possible when the data transfer process is simplified.

These indicate that further work is still remaining. First, linearization of the plant model may use other methods and this may achieve a better working range for the control system. Second, the decoupling methods attempted in this thesis may not be the most ideal to manipulate the multivariable system under study. Applying of other methods may give a more desirable result.

On the whole, the temperature and level of the target tank can be adjusted to the user's setpoints through the RT-Lab system. These process variables can remain at steady values with only small deviations from the desired values, which proves the designed control system to be successful.

References

[1] Pierre R. Bélanger, *Control Engineering: A Modern Approach*, Saunders College Publishing 1995

[2] Benoit Boulet, *Linear System (McGill University ECE501) Course Notes*

[3] Graham C. Goodwin, *Control System Design*, Prentice Hall 2000

[4] K. Warwick, D. Rees, *Industrial Digital Control Systems*, IEEE Control Engineering Series 37. 1988

[5] Jane W.S. Liu, *Real-Time Systems*, Printice Hall 2000

[6] Ynnus A. Cengel, Michael A. Boles, *Thermodynamics: An engineering Approach 2nd Edition*, McGraw-Hill, Inc. 1994

[7] J.P.Holman, *Heat Transfer 8th edition*, McGraw-Hill, Inc 1997

[8] W. Roezel, Y. Xuan, *Dynamic behaviour of Heat Exchangers*, WIT Press 1999

[9] S. Kakac, H. Liu, *Heat Exchangers*, CRC Press 1998

[10] Katsuhiko Ogata, *Modern Control Engineering 3rd edition,* Prentice Hall 1998

[11] Krishna Singh and Gayatri Agnihotri, *System design through MATLAB, Control Toolbox and SIMULINK*, London ; New York : Springer, 2001.

[12] Muhammad H. Rashid, *Microelectronic circuits : analysis and design*, PWS Pub., 1999

[13] Ramón Pallás-Areny, John G. Webster, *Analog signal processing*, Wiley Pub., 1999

[14] K. Warwick, D. Rees, *Industrial Digital Control Systems*, IEEE Control Engineering Series 37. 1988

[15] George Zames and David Bensoussan, Multivariable Feedback, Sensitivity, and Decentralized Control, IEEE Transactions on Automatic Control, Vol. AC-28, NO11.

Appendix A

Matlab Program for heat exchanger system modeling and analisys.

```
  Heat Exchanger System Modeling and Analisys V 5.3
  by Shuo Liu
%
% 1) Calculate the equilibrium Points for the nonlinear systemmodel.
% 2) Calculate the parameters for the linearized model
% 3) Analysis of the linearized model
% 4) Calculate the Transfer Function of the Linearized model
% 5) Decoupling Network analysis based on the derived transfer function
% 6) RGA Analysis based on the derived transfer function
% 7) Generate step function at arbitrary final value
% 8) Generate step response of the linearized model



clear all;

%**********Parameters Required in State Space Model**********

%**********Parameters Required in Water Tank Model**********
Area = 0.0198-0.0001131*2-0.00038;   % Cross Section Area (m^2)
hr = 0.005;                          %  Orrifice's Radius (m)
a1 = pi*hr*hr;                       % Orrifice's Cross Section (m^2)
g = 9.81;                            %(m/sec^2)
he = 0.05                            % Operation Level of Target Tank (m)

%**********Parameters Required in Heat Exchanger Model**********
alpha=0.9               % Heat Loss Constant
k=200000/60               % Heat Transfer Coefficient( j/sec*c)
rho=1000                % Water Density(kg/m^3)
Cv=4180                 % Water Heat Capacity(J/Kg*C)
Vc=0.00005028/2         % Primary Water Sub-Section Volume(m^3)
Vh=0.000098691/2        % Secondary Water Sub-Section Volume(m^3)
Fc = 0.004225/60          % Primary Water Flow Rate(Maximun) (m^3/sec)
Fh = 0.00094635/60        % Primary Water Flow Rate(Maximun) (m^3/sec)
Tc0=22                  % Temperature of the Water Flowing Into First Cold Tank (C)
Th0=55                  % Temperature of the Water Flowing Into First Hot Tank (C)

A1=alpha*k/rho*Vc*Cv
A2=k/rho*Vc*Cv
A3=1/Vc
A4=1/Vh



%**********Calculating the Equlibrium Flow rate**********
Ue = 0.003/60                          % Operation Flow Rate (M^3/sec)

Ae = -3.3181                          % Matrix A of the linearized model


%**********Calculating the Equlibrium Temperature**********

u1 = Ue             % Operation Point of Primary Water Flow
u2 = Fh/2               % Operation Point of Secondary Water Flow
U=[u1;u2]
```

```
 = [-(A3*u1+A1)          0          0          A1          ;
    A3*u1       -(A3*u1+A1)         A1          0          ;
     0                  A2      -(A4*u2+A2)     0          ;
     A2                 0          A4*u2      -(A4*u2+A2)   ;]

B= [A3*Tc0*u1; 0; A4*Th0*u2; 0]

C= [0 1 0 0]

D = [0 0]

X = A\(-B)              % Calculating the Equlibrium Point

Result=A*X+B            % Check if the calculated is indeed the equlibrium

%***********Linearized System Model (SISO)*************

deltaA1 =  [-(A3*u1+A1)          0                  0                  A1          ;
           A3*u1                -(A3*u1+A1)         A1                 0          ;
           0                    A2                 -(A4*u2+A2)        0          ;
           A2                   0                   A4*u2             -(A4*u2+A2)  ;
]


deltaB1 =  [A3*Tc0-A3*X(1)        0;
           A3*X(1)-A3*X(2)        0;
           0                     A4*Th0-A4*X(3)
           0                     A4*X(3)-A4*X(4)]



deltaC1 = [0 1 0 0 ;
           0 0 0 0 ;]

deltaD1 =[0]

hxsys1= ss(deltaA1,deltaB1,deltaC1,deltaD1)  % Get the Linearized model

%***********Analysis of Linearized System*************

EigenA=eig(deltaA1)

con=ctrb(deltaA1,deltaB1)

cbility  = rank(con)                    % Rank of the controllablity matrix

pzmap (hxsys1)

%***********Linearized System Model (MIMO)*************

deltaA =  [-(A3*u1+A1)          0                  0                  A1          0;
           A3*u1                -(A3*u1+A1)         A1                 0          0;
           0                    A2                 -(A4*u2+A2)        0          0;
           A2                   0                   A4*u2             -(A4*u2+A2)  0;
           0                    0                   0                  0          -3.3181;]
```

```
 eltaB =  [A3*Tc0-A3*X(1)          0;
           A3*X(1)-A3*X(2)          0;
           0                       A4*Th0-A4*X(3)
           0                       A4*X(3)-A4*X(4)
           52.102                  0;]



deltaC=[0 1 0 0 0;
        0 0 0 0 1;]

deltaD=[0 0;
        0 0;]

hxsys= ss(deltaA,deltaB,deltaC,deltaD)  % Get the Linearized model



% %***********Analysis of Linearized System**************
%
% EigenA=eig(deltaA)
%
% con=ctrb(deltaA,deltaB)
%
% cbility  = rank(con)                    % Rank of the controllablity matrix
%
% pzmap (hxsys)
%
% pole = pole(hxsys)
%
% zero = zero(hxsys)

%************Transfer Function***************

Gs=tf(hxsys)

Gs11 =  tf(Gs(1,1));
Gs12 =  tf(Gs(1,2));
Gs21 =  tf(Gs(2,1));
Gs22 =  tf(Gs(2,2));

% pzmap (Gs12);
% figure
% pzmap (Gs21);

[Gs11num,Gs11den] = TFDATA(Gs11, 'v')
[Gs12num,Gs12den] = TFDATA(Gs12, 'v')
[Gs21num,Gs21den] = TFDATA(Gs21, 'v')
[Gs22num,Gs22den] = TFDATA(Gs22, 'v')

%************Decoupling Network ***************
%
% [Gd12num,Gd12den] = TFDATA((-1*Gs12/Gs11), 'v')
% [Gd21num,Gd21den] = TFDATA((-1*Gs21/Gs22), 'v')

 k11 = dcgain(Gs11);
```

```
 k12 = dcgain(Gs12);
 k21 = dcgain(Gs21);
 k22 = dcgain(Gs22);

%  E12 =  k12/k22;
%  E21 =  k21/k11;

%************RGA Analysis***************
Gdc = [k11, k12;
       k21, k22];

 Gdci= inv(Gdc);


 Lamda(1,1) = Gdc(1,1)*Gdci(1,1);
 Lamda(1,2) = Gdc(1,2)*Gdci(2,1);
 Lamda(2,1) = Gdc(2,1)*Gdci(1,2);
 Lamda(2,2) = Gdc(2,2)*Gdci(2,2);


%************Gennerate Step Signal***************

%Cold Water Flow Step Signal
stepsignal = [0.1:0.1:10]

for time = 1:1:101;
    if time <= 10;
       stepsignal(time) = 0;
    else stepsignal(time) = Fc/8;
    end;
end;
stept = [0:1:100]

%Hot Water Flow Step Signal

for time2 = 1:1:101;
    if time2 <= 10;
       stepsignal2(time2) = 0;
    else stepsignal2(time2) = Fh;
    end;
end;

%************Step Response***************

stepsignal = [stepsignal;stepsignal2];

LSIM(hxsys,stepsignal,stept);

% figure;

% LSIM(Gs,stepsignal,stept);
```